Computer Methods in Applied Mechanics and Engineering 454 (2026) 118845

Contents lists available at ScienceDirect

Comput. Methods Appl. Mech. Engrg.

journal homepage: www.elsevier.com/locate/cma

Toward uncertainty quantification with arbitrarily dependent probability distributions of random input

Md Rashel Talukdar [1], Sharif Rahman [2,*]

Department of Mechanical Engineering, The University of Iowa, Iowa City, IA, 52242, USA

ARTICLE INFO

Keywords:
Generalized polynomial dimensional decomposition
Multivariate orthogonal polynomials
Reliability analysis
Second-moment analysis
Whitening transformation

ABSTRACT

This paper puts forward a novel and practical adaptation of generalized polynomial dimensional decomposition (GPDD) for uncertainty quantification (UQ) in the presence of dependent input random variables with arbitrary, non-product-type probability distributions. Instead of relying on a Rodrigues-type formula, which exists only for select probability measures, a new four-step computational algorithm is introduced to generate approximate, measure-consistent multivariate orthogonal polynomials in subsets of input variables. Unlike generalized polynomial chaos expansion (GPCE), which requires the full joint input distribution to construct its orthogonal polynomial basis, GPDD operates using only low-variate marginal distributions, allowing efficient dimensionwise construction even when the joint distribution is unknown. For high-dimensional stochastic problems characterized by strongly nonlinear output but weak input interactions, GPDD is expected to deliver substantial computational advantages over GPCE due to its hierarchical, dimensionwise structure. Numerical experiments involving both Gaussian and non-Gaussian probability measures on rectangular and non-rectangular domains show that the proposed algorithm produces highly accurate orthogonal polynomials. Results from representative mathematical and structural examples demonstrate that GPDD provides accurate and computationally efficient estimates of statistical moments and reliability, while an engineering application involving stochastic stress analysis of a vehicle suspension control arm with 34 random variables further highlights GPDD's practical effectiveness for high-dimensional UQ problems.

1. Introduction

Uncertainty quantification (UQ) plays a pivotal role in the mathematical modeling, simulation, and design of complex mechanical systems. Contemporary UQ techniques, often employed as surrogates for computationally intensive models, include polynomial chaos expansion (PCE) [1,2], adaptive-sparse PCE [3], polynomial dimensional decomposition (PDD) [4,5], stochastic collocation [6,7], and sparse-grid quadrature [8,9], among others. These methods are widely recognized for offering significant computational advantages over crude Monte Carlo simulation (MCS).

However, a key limitation shared by most of these approaches is their reliance on the assumption of statistical independence among input random variables. In many practical applications, this assumption is violated, as input variables, arising from loading conditions, geometric configurations, or material properties, are often correlated or otherwise statistically dependent. Neglecting

* Corresponding author.
E-mail addresses: mdrashel-talukdar@uiowa.edu (M.R. Talukdar), sharif-rahman@uiowa.edu (S. Rahman).
[1] Graduate Student.
[2] Professor.

https://doi.org/10.1016/j.cma.2026.118845
Received 14 December 2025; Received in revised form 3 February 2026; Accepted 11 February 2026
Available online 26 February 2026

such dependencies can lead to inaccurate predictions of probabilistic response characteristics, potentially resulting in suboptimal or unsafe designs [10]. To address this issue, measure transformations like the Rosenblatt transformation [11] are commonly used to convert dependent input variables into independent counterparts, thereby enabling the application of traditional methods, such as PCE [12,13] and others. However, these transformations often introduce significant nonlinearity into the input-output relationships of stochastic systems, thereby impairing the convergence properties of the resulting probabilistic solutions. Consequently, there is a compelling need for the development of novel methodologies or the enhancement of existing ones that can effectively perform UQ analysis in the presence of arbitrary dependence among input variables.

Recent advances in UQ have introduced generalized versions of PCE or PDD capable of handling statistically dependent input variables through Fourier-like series expansions with respect to measure-consistent multivariate orthonormal or orthogonal polynomials [14–17]. In addition, data-driven PCE approaches have been proposed to address high-dimensional dependent input by learning low-dimensional representations from data [18]. These methods avoid potentially degrading measure transformations between dependent and independent variables, offering a promising direction for general UQ analysis. However, their broader applicability is limited by two major challenges: (1) generating orthogonal polynomials consistent with arbitrary input distributions is generally infeasible analytically [19] or numerically unstable in high dimensions using methods like Gram-Schmidt [20]; and (2) computing the expansion coefficients requires evaluating high-dimensional integrals, which are typically intractable analytically and prohibitively expensive via tensor-product quadrature. Addressing these two limitations is essential for enabling practical UQ analyses under arbitrary dependence structures and constitutes the central motivation of this work.

The primary objective of this study is to develop a constructive framework of the generalized PDD, hereafter referred to as GPDD, for UQ analysis of complex systems subject to arbitrary, statistically dependent probability distributions of input variables. While the present work focuses on the practical implementation of GPDD, readers seeking a deeper understanding of its mathematical foundations are referred to the companion papers [15,16]. The structure of this paper is as follows. Section 2 introduces the mathematical notation and preliminaries, along with a set of essential assumptions. Section 3 outlines a new four-step algorithm for the construction of measure-consistent multivariate orthogonal polynomials in subsets of input variables. Section 4 presents the GPDD formulation and its truncated form, including the expressions for estimating second-moment properties of a general output variable and associated reliability analysis. Section 5 details a procedure for constructing approximate orthogonal polynomials and standard least-squares regression for estimating the expansion coefficients, leading to a practical, implementable version of GPDD. Numerical results for three representative example problems are presented in Section 6. Section 7 addresses a large-scale engineering application involving the probabilistic analysis of a lower control arm in an automotive suspension system, thereby demonstrating the practical applicability and effectiveness of the GPDD method developed in this study. Section 8 discusses potential directions for future research, and concluding remarks are provided in Section 9.

2. A general UQ problem involving dependent variables

Let $\mathbb{N} := \{1, 2, \ldots\}$, $\mathbb{N}_0 := \mathbb{N} \cup \{0\}$, $\mathbb{R} := (-\infty, +\infty)$, and $\mathbb{R}_0^+ := [0, +\infty)$ represent the sets of positive integer (natural), non-negative integer, real, and non-negative real numbers, respectively. For a finite integer $N \in \mathbb{N}$, denote by $\mathbb{A}^N \subseteq \mathbb{R}^N$ a bounded or unbounded subdomain of $\mathbb{R}^N$.

2.1. Input random variables

Let $(\Omega, \mathcal{F}, \mathbb{P})$ be a complete probability triple, where Ω is a sample space representing an abstract set of elementary events, $\mathcal{F}$ is a σ-algebra on Ω, and $\mathbb{P} : \mathcal{F} \to [0, 1]$ is a probability measure. With $\mathcal{B}^N := \mathcal{B}(\mathbb{A}^N)$ representing the Borel σ-algebra on $\mathbb{A}^N \subseteq \mathbb{R}^N$, consider an $\mathbb{A}^N$-valued random vector $\mathbf{X} := (X_1, \ldots, X_N)^\intercal : (\Omega, \mathcal{F}) \to (\mathbb{A}^N, \mathcal{B}^N)$, describing the statistical uncertainties in all input and system parameters of a stochastic or UQ problem. Every so often, $\mathbf{X}$ will be referred to as an input random vector or variables, and the integer N, representing the total number of input random variables, will be designated as the stochastic dimension of the UQ problem. As an example, consider a cantilever beam, which has the following input parameters: (1) a random length L; (2) a prismatic rectangular cross-section with a random depth H and a random width W; (3) a random Young's modulus E; and (4) a random concentrated load F. If all of these input parameters are modeled as random variables, then the UQ problem involves an input random vector $\mathbf{X} := (L, H, W, E, F)^\intercal$ with stochastic dimension $N = 5$.

Denote by $F_{\mathbf{X}}(\mathbf{x}) := \mathbb{P}\left[\cap_{i=1}^N \{X_i \le x_i\}\right]$ the joint cumulative probability distribution function (CDF) of $\mathbf{X}$, admitting the joint probability density function (PDF) $f_{\mathbf{X}}(\mathbf{x}) := \partial^N F_{\mathbf{X}}(\mathbf{x})/\partial x_1 \cdots \partial x_N$. Given the abstract probability space $(\Omega, \mathcal{F}, \mathbb{P})$, the image probability space is $(\mathbb{A}^N, \mathcal{B}^N, f_{\mathbf{X}} d\mathbf{x})$, where $\mathbb{A}^N$ can be viewed as the image of Ω from the mapping $\mathbf{X} : \Omega \to \mathbb{A}^N$, and is also the support of $f_{\mathbf{X}}(\mathbf{x})$.

A set of requisite assumptions for UQ analysis conducted is as follows.

Assumption 1. The input random vector $\mathbf{X} := (X_1, \ldots, X_N)^T : (\Omega, \mathcal{F}) \to (\mathbb{A}^N, \mathcal{B}^N)$

1. has an absolutely continuous joint CDF $F_{\mathbf{X}}(\mathbf{x})$ and a continuous joint PDF $f_{\mathbf{X}}(\mathbf{x})$ with a bounded or unbounded support $\mathbb{A}^N \subseteq \mathbb{R}^N$;
2. possesses absolute finite moments of all orders, that is, for all $\mathbf{j} := (j_1, \ldots, j_N) \in \mathbb{N}_0^N$,

$$\mathbb{E}\left[|\mathbf{X}^{\mathbf{j}}|\right] := \int_\Omega |\mathbf{X}^{\mathbf{j}}(\omega)| d\mathbb{P}(\omega) = \int_{\mathbb{A}^N} |\mathbf{x}^{\mathbf{j}}| f_{\mathbf{X}}(\mathbf{x}) d\mathbf{x} < \infty, \tag{1}$$

   where $\mathbf{X}^{\mathbf{j}} = X_1^{j_1} \cdots X_N^{j_N}$ and $\mathbb{E}$ is the expectation operator with respect to the probability measure $\mathbb{P}$ or $f_{\mathbf{X}}(\mathbf{x})d\mathbf{x}$;
3. has a joint PDF $f_{\mathbf{X}}(\mathbf{x})$, which

(a) has a compact support, that is, there exists a compact subset $\mathbb{A}^N \subset \mathbb{R}^N$ such that $\mathbb{P}(\mathbf{X} \in \mathbb{A}^N) = 1$, or
(b) is exponentially integrable, that is, there exists a real number $a > 0$ such that

$$\int_{\mathbb{A}^N} \exp(a\|\mathbf{x}\|) f_{\mathbf{X}}(\mathbf{x}) d\mathbf{x} < \infty, \tag{2}$$

where $\|\cdot\| : \mathbb{A}^N \to \mathbb{R}_0^+$ is an arbitrary norm; and

4. has a joint PDF $f_{\mathbf{X}}(\mathbf{x})$ with a grid-closed support, that is, there exists a grid for every point $\mathbf{x}$ of $\text{supp}(f_{\mathbf{X}}) = \mathbb{A}^N \subseteq \mathbb{R}^N$.

Assumption 1 imposes mild conditions that are commonly satisfied in practical UQ applications. For a comprehensive discussion and formal justification of this assumption, readers are referred to the foundational works on GPDD [15,16].

2.2. Output random variable

Given an input random vector $\mathbf{X} := (X_1, \ldots, X_N)^\intercal : (\Omega, \mathcal{F}) \to (\mathbb{A}^N, \mathcal{B}^N)$ with known PDF $f_{\mathbf{X}}(\mathbf{x})$ on $\mathbb{A}^N \subseteq \mathbb{R}^N$, denote by $y(\mathbf{X}) := y(X_1, \ldots, X_N)$ a real-valued, square-integrable, measurable transformation on $(\Omega, \mathcal{F})$. Here, $y : \mathbb{A}^N \to \mathbb{R}$ represents a relevant function from a mathematical model, describing an output response of interest for a UQ problem. A major objective of UQ analysis is to estimate the probabilistic characteristics of an output random variable $Y = y(\mathbf{X})$, including statistical moments and reliability, when the probability law of the input random vector $\mathbf{X}$ is prescribed. More often than not, Y is assumed to belong to a reasonably large class of random variables, such as the weighted L^2 space

$$L^2(\Omega, \mathcal{F}, \mathbb{P}) := \left\{ Y : \Omega \to \mathbb{R} : \int_\Omega |y(\mathbf{X}(\omega))|^2 d\mathbb{P}(\omega) = \int_{\mathbb{A}^N} |y(\mathbf{x})|^2 f_{\mathbf{X}}(\mathbf{x}) d\mathbf{x} < \infty \right\},$$

which is a Hilbert space with the inner product

$$(y(\mathbf{X}), z(\mathbf{X}))_{L^2(\Omega,\mathcal{F},\mathbb{P})} := \int_\Omega y(\mathbf{X}(\omega)) z(\mathbf{X}(\omega)) d\mathbb{P}(\omega) = \int_{\mathbb{A}^N} y(\mathbf{x}) z(\mathbf{x}) f_{\mathbf{X}}(\mathbf{x}) d\mathbf{x}$$

and norm

$$\|y(\mathbf{X})\|_{L^2(\Omega,\mathcal{F},\mathbb{P})} := \sqrt{(y(\mathbf{X}), y(\mathbf{X}))_{L^2(\Omega,\mathcal{F},\mathbb{P})}} = \sqrt{\int_\Omega y^2(\mathbf{X}(\omega)) d\mathbb{P}(\omega)} = \sqrt{\int_{\mathbb{A}^N} y^2(\mathbf{x}) f_{\mathbf{X}}(\mathbf{x}) d\mathbf{x}}.$$

It is elementary to show that $y(\mathbf{X}(\omega)) \in L^2(\Omega, \mathcal{F}, \mathbb{P})$ if and only if $y(\mathbf{x}) \in L^2(\mathbb{A}^N, \mathcal{B}^N, f_{\mathbf{X}} d\mathbf{x})$.

3. Measure-consistent, dimensionwise multivariate orthogonal polynomials

When $\mathbf{X} = (X_1, \ldots, X_N)^\intercal$ consists of statistically dependent random variables, its joint PDF cannot be decomposed into a product of its marginal PDFs. As a result, multivariate orthogonal polynomial basis functions that are consistent with the probability measure of $\mathbf{X}$ cannot, in general, be formed by an N-dimensional tensor product of univariate orthogonal polynomial basis functions [19,21–24]. For certain probability measures with infinitely differentiable PDFs, Rodrigues-type formulas exist, enabling the derivation of multivariate orthogonal polynomials from derivatives of the PDF [15,19,21,25]. However, no such formula is available for a general probability measure, necessitating alternative construction methods, such as the Gram-Schmidt procedure or three-term recurrence relations. More importantly, if the stochastic dimension N is high (*e.g.*, $N \geq 10$), the number of basis functions grows rapidly, even for relatively low polynomial orders. Alternatively, to suppress rapid proliferation of basis functions, measure-consistent orthogonal polynomials can be developed in subsets of input variables. This section introduces a new, general four-step algorithm to construct such multivariate orthogonal polynomials in a dimensionwise manner.

3.1. A four-step algorithm

For $N \in \mathbb{N}$, denote by $\{1, \ldots, N\}$ an index set, so that $u \subseteq \{1, \ldots, N\}$ is a subset, including the empty set $\emptyset$, with cardinality $0 \leq |u| \leq N$. The complementary subset of u is denoted by $-u := \{1, \ldots, N\} \backslash u$. For $\emptyset \neq u \subseteq \{1, \ldots, N\}$, let $\mathbf{X}_u := (X_{i_1}, \ldots, X_{i_{|u|}})^\intercal$, $1 \leq i_1 < \cdots < i_{|u|} \leq N$, a subvector of $\mathbf{X}$, be defined on the abstract probability space $(\Omega^u, \mathcal{F}^u, \mathbb{P}^u)$, where Ω^u is the sample space of $\mathbf{X}_u$, $\mathcal{F}^u$ is a σ-algebra on Ω^u, and $\mathbb{P}^u$ is a probability measure. The complementary subvector is defined by $\mathbf{X}_{-u} := \mathbf{X}_{\{1,\ldots,N\}\backslash u}$. The corresponding image probability space is $(\mathbb{A}^u, \mathcal{B}^u, f_{\mathbf{X}_u} d\mathbf{x}_u)$, where $\mathbb{A}^u \subseteq \mathbb{R}^{|u|}$ is the image sample space of $\mathbf{X}_u$, $\mathcal{B}^u$ is the Borel σ-algebra on $\mathbb{A}^u$, and

$$f_{\mathbf{X}_u}(\mathbf{x}_u) := \int_{\mathbb{A}^{-u}} f_{\mathbf{X}}(\mathbf{x}) d\mathbf{x}_{-u}$$

is the marginal PDF of $\mathbf{X}_u$ supported on $\mathbb{A}^u$.

When $\emptyset \neq u \subseteq \{1, \ldots, N\}$, a $|u|$-dimensional multi-index is denoted by $\mathbf{j}_u := (j_{i_1}, \ldots, j_{i_{|u|}}) \in \mathbb{N}_0^{|u|}$ with the total degree $|\mathbf{j}_u| := j_{i_1} + \cdots + j_{i_{|u|}}$, where $j_{i_p} \in \mathbb{N}_0$, $p = 1, \ldots, |u|$, represents the pth component of $\mathbf{j}_u$.[1]

The proposed four-step algorithm to generate multivariate orthogonal polynomials that are consistent with the probability measure $f_{\mathbf{X}_u}(\mathbf{x}_u) d\mathbf{x}_u$ of $\mathbf{X}_u$ is described in the following four subsections.

[1] The same symbol $|\cdot|$ is used for denoting both the cardinality of a set and the degree of a multi-index in this paper.

3.1.1. Step 1: Monomial basis

For $\mathbf{x}_u = (x_{i_1}, \dots, x_{i_{|u|}})^\intercal \in \mathbb{A}^u \subseteq \mathbb{R}^{|u|}$, a monomial in the real variables $x_{i_1}, \dots, x_{i_{|u|}}$ is the product

$$\mathbf{x}_u^{\mathbf{j}_u} = x_{i_1}^{j_{i_1}} \cdots x_{i_{|u|}}^{j_{i_{|u|}}}$$

and has a total degree $|\mathbf{j}_u|$. Given $\emptyset \neq u \subseteq \{1, \dots, N\}$ and $|u| \leq m < \infty$, define two multi-index sets

$$\mathcal{I}_{u,m} := \left\{ \mathbf{j}_u \in \mathbb{N}_0^{|u|} : 0 \leq |\mathbf{j}_u| \leq m \right\}$$

and

$$\bar{\mathcal{I}}_{u,m} := \left\{ \mathbf{j}_u \in \mathbb{N}^{|u|} : |u| \leq |\mathbf{j}_u| \leq m \right\} \subsetneq \mathcal{I}_{u,m}$$

with cardinalities

$$L_{u,m} := |\mathcal{I}_{u,m}| = \binom{|u|+m}{m} = \frac{(|u|+m)!}{|u|!\, m!} \tag{3}$$

and

$$\bar{L}_{u,m} := |\bar{\mathcal{I}}_{u,m}| = \sum_{l=|u|}^{m} \binom{l-1}{|u|-1} = \sum_{l=|u|}^{m} \frac{(l-1)!}{(|u|-1)!\,(l-|u|)!}, \tag{4}$$

respectively. Here, the lowest possible value of each component of $\mathbf{j}_u$ is *zero* in $\mathcal{I}_{u,m}$, while it is *one* in $\bar{\mathcal{I}}_{u,m}$. Therefore, $\bar{\mathcal{I}}_{u,m}$ is a proper subset of $\mathcal{I}_{u,m}$, representing a reduced index set.

Associated with the index set $\mathcal{I}_{u,m}$ or $\cup_{v \subseteq u} \bar{\mathcal{I}}_{v,m}$, define a set of monomials

$$\mathcal{B}_{u,m} := \left\{ \mathbf{x}_u^{\mathbf{j}_u} : \mathbf{j}_u \in \mathcal{I}_{u,m} \right\} = \bigcup_{v \subseteq u} \left\{ \mathbf{x}_v^{\mathbf{j}_v} : \mathbf{j}_v \in \bar{\mathcal{I}}_{v,m} \right\} = \left\{ \mathbf{x}_u^{\mathbf{j}_u^{(1)}}, \dots, \mathbf{x}_u^{\mathbf{j}_u^{(i)}}, \dots, \mathbf{x}_u^{\mathbf{j}_u^{(L_{u,m})}} \right\} \tag{5}$$

in $\mathbf{x}_u$ of degree at most m. Here, the second equality indicates that $\mathcal{B}_{u,m}$ can also be constructed from the union of monomials in all subsets of u of degree at most m. In the third equality, the monomial basis functions have been arranged according to an order of choice, where $\mathbf{x}_u^{\mathbf{j}_u^{(i)}}$ represents the ith basis. It is well known that the set $\mathcal{B}_{u,m}$ constitutes a basis of the vector space

$$\Pi_{u,m} := \text{span}\left\{ \mathcal{B}_{u,m} \right\}, \ |u| \leq m < \infty,$$

of polynomials in $\mathbf{x}_u$ of degree at most m.

3.1.2. Step 2: Local monomial vector

From the monomial basis $\mathcal{B}_{u,m}$ in (5), select a kth monomial element $\mathbf{x}_u^{\mathbf{j}_u^{(k)}}$, $\mathbf{j}_u^{(k)} = (j_{i_1}^{(k)}, \dots, j_{i_{|u|}}^{(k)})$, such that $1 \leq j_{i_p}^{(k)} \leq m$, $p = 1, \dots, |u|$, and $|u| \leq |\mathbf{j}_u^{(k)}| \leq m$. There are $\bar{L}_{u,m}$ such elements in $\mathcal{B}_{u,m}$, as determined by (4). Given u and $\mathbf{j}_u^{(k)}$ of the kth monomial, the reduced multi-index set

$$\mathcal{I}_{u,|\mathbf{j}_u^{(k)}|} := \left\{ \mathbf{j}_u \in \mathcal{I}_{u,m} : 0 \leq |\mathbf{j}_u| \leq |\mathbf{j}_u^{(k)}| \right\} \subseteq \mathcal{I}_{u,m}$$

contains specific multi-index values such that all associated monomials $\mathbf{x}_u^{\mathbf{j}_u}$ have degrees less than or equal to $|\mathbf{j}_u^{(k)}| \leq m$. It has cardinality

$$L_{u,|\mathbf{j}_u^{(k)}|} := |\mathcal{I}_{u,|\mathbf{j}_u^{(k)}|}| = \binom{|u|+|\mathbf{j}_u^{(k)}|}{|\mathbf{j}_u^{(k)}|}.$$

Hereafter, by introducing another multi-index $\mathbf{l}_u \in \mathcal{I}_{u,|\mathbf{j}_u^{(k)}|}$, arrange the elements of $\mathcal{I}_{u,|\mathbf{j}_u^{(k)}|}$ as

$$\mathcal{I}_{u,|\mathbf{j}_u^{(k)}|} = \left\{ \mathbf{l}_u^{(1)}, \dots, \mathbf{l}_u^{(L_{u,|\mathbf{j}_u^{(k)}|})} \right\}, \ \mathbf{l}_u^{(1)} = \mathbf{0}, \ \mathbf{l}_u^{(L_{u,|\mathbf{j}_u^{(k)}|})} = \mathbf{j}_u^{(k)},$$

leading to a reduced basis set

$$\mathcal{B}_{u,\mathbf{j}_u^{(k)}} := \left\{ \mathbf{x}_u^{\mathbf{l}_u} : \mathbf{l}_u \in \mathcal{I}_{u,|\mathbf{j}_u^{(k)}|} \right\} = \left\{ \begin{matrix} \mathbf{x}_u^{\mathbf{l}_u^{(1)}}, \dots, \mathbf{x}_u^{\mathbf{l}_u^{(L_{u,|\mathbf{j}_u^{(k)}|}-1)}}, \mathbf{x}_u^{\mathbf{l}_u^{(L_{u,|\mathbf{j}_u^{(k)}|})}} \end{matrix} \right\}, \ \mathbf{x}_u^{\mathbf{l}_u^{(1)}} = 1, \ \mathbf{x}_u^{\mathbf{l}_u^{(L_{u,|\mathbf{j}_u^{(k)}|})}} = \mathbf{x}_u^{\mathbf{j}_u^{(k)}}, \tag{6}$$

where, in the second equality, the monomials have been arranged such that the first element is 1 and the last element is $\mathbf{x}_u^{\mathbf{j}_u^{(k)}}$. Then, using the elements of $\mathcal{B}_{u,|\mathbf{j}_u^{(k)}|}$, define an $L_{u,|\mathbf{j}_u^{(k)}|}$-dimensional column vector

$$\mathbf{P}_{u,\mathbf{j}_u^{(k)}}(\mathbf{x}_u) := \left(\begin{matrix} \mathbf{x}_u^{\mathbf{l}_u^{(1)}}, \dots, \mathbf{x}_u^{\mathbf{l}_u^{(L_{u,|\mathbf{j}_u^{(k)}|}-1)}}, \mathbf{x}_u^{\mathbf{l}_u^{(L_{u,|\mathbf{j}_u^{(k)}|})}} \end{matrix} \right)^\intercal, \ \mathbf{x}_u^{\mathbf{l}_u^{(1)}} = 1, \ \mathbf{x}_u^{\mathbf{l}_u^{(L_{u,|\mathbf{j}_u^{(k)}|})}} = \mathbf{x}_u^{\mathbf{j}_u^{(k)}}, \tag{7}$$

of local monomials associated with the kth monomial element of $\mathcal{B}_{u,m}$. Here, $\mathbf{P}_{u,\mathbf{j}_u^{(k)}}(\mathbf{x}_u)$ is referred to as the kth local monomial vector.

3.1.3. Step 3: Moment matrix

When the input random variables $X_{i_1}, \dots, X_{i_{|u|}}$, instead of the real variables $x_{i_1}, \dots, x_{i_{|u|}}$, are inserted in the argument, the local monomial vector $\mathbf{P}_{u,\mathbf{j}_u^{(k)}}(\mathbf{X}_u)$ becomes a vector of random monomials. This leads to a $(L_{u,|\mathbf{j}_u^{(k)}|} \times L_{u,|\mathbf{j}_u^{(k)}|})$ moment matrix of $\mathbf{P}_{u,\mathbf{j}_u^{(k)}}(\mathbf{X}_u)$, defined as

$$\mathbf{G}_{u,\mathbf{j}_u^{(k)}} := \mathbb{E}\left[\mathbf{P}_{u,\mathbf{j}_u^{(k)}}(\mathbf{X}_u)\mathbf{P}^{\intercal}_{u,\mathbf{j}_u^{(k)}}(\mathbf{X}_u)\right] := \int_{\mathbb{A}^u} \mathbf{P}_{u,\mathbf{j}_u^{(k)}}(\mathbf{x}_u)\mathbf{P}^{\intercal}_{u,\mathbf{j}_u^{(k)}}(\mathbf{x}_u) f_{\mathbf{X}_u}(\mathbf{x}_u) d\mathbf{x}_u, \tag{8}$$

with its (p,q)th element

$$G_{u,\mathbf{j}_u^{(k)},pq} := \mathbb{E}[\mathbf{X}_u^{\mathbf{j}_u^{(p)}} \mathbf{X}_u^{\mathbf{j}_u^{(q)}}] := \int_{\mathbb{A}^u} \mathbf{x}^{\mathbf{j}_u^{(p)}} \mathbf{x}_u^{\mathbf{j}_u^{(q)}} f_{\mathbf{X}_u}(\mathbf{x}_u) d\mathbf{x}_u = \int_{\mathbb{A}^u} \mathbf{x}_u^{\mathbf{j}_u^{(p)}+\mathbf{j}_u^{(q)}} f_{\mathbf{X}_u}(\mathbf{x}_u) d\mathbf{x}_u, \quad p,q = 1, \dots, L_{u,|\mathbf{j}_u^{(k)}|}. \tag{9}$$

It is elementary to show that $\mathbf{G}_{u,\mathbf{j}_u^{(k)}}$ is a Gram matrix and hence symmetric and positive-definite.

3.1.4. Step 4: Whitening transformation

Denote by $\Psi_{u,\mathbf{j}_u^{(k)}}(\mathbf{x}_u)$ the kth orthogonal polynomial counterpart of the kth monomial $\mathbf{x}_u^{\mathbf{j}_u^{(k)}}$. Such a polynomial can be determined from the local monomial vector $\mathbf{P}_{u,\mathbf{j}_u^{(k)}}(\mathbf{x}_u)$ and properties of the moment matrix $\mathbf{G}_{u,\mathbf{j}_u^{(k)}}$, where the orthogonality is addressed in Section 3.2. Since the monomial moment matrix $\mathbf{G}_{u,\mathbf{j}_u^{(k)}}$ is symmetric and positive-definite, it is invertible. Therefore, there exists a non-singular $(L_{u,|\mathbf{j}_u^{(k)}|} \times L_{u,|\mathbf{j}_u^{(k)}|})$ whitening matrix $\mathbf{W}_{u,\mathbf{j}_u^{(k)}}$ (say), satisfying

$$\mathbf{W}^{\intercal}_{u,\mathbf{j}_u^{(k)}} \mathbf{W}_{u,\mathbf{j}_u^{(k)}} = \mathbf{G}^{-1}_{u,\mathbf{j}_u^{(k)}} \quad \text{or} \quad \mathbf{W}^{-1}_{u,\mathbf{j}_u^{(k)}} \mathbf{W}^{-\intercal}_{u,\mathbf{j}_u^{(k)}} = \mathbf{G}_{u,\mathbf{j}_u^{(k)}}. \tag{10}$$

Thereafter, apply a whitening transformation to create the kth orthogonal polynomial as

$$\Psi_{u,\mathbf{j}_u^{(k)}}(\mathbf{x}_u) = \mathbf{e}^{\intercal}_{L_{u,|\mathbf{j}_u^{(k)}|}} \mathbf{W}_{u,\mathbf{j}_u^{(k)}} \mathbf{P}_{u,\mathbf{j}_u^{(k)}}(\mathbf{x}_u), \tag{11}$$

where $\mathbf{e}_{L_{u,|\mathbf{j}_u^{(k)}|}} := (0, \dots, 1)^{\intercal}$ is an $L_{u,|\mathbf{j}_u^{(k)}|}$-dimensional standard unit vector employed here to pick the last row of the matrix-vector multiplication. However, the whitening matrix $\mathbf{W}_{u,\mathbf{j}_u^{(k)}}$ involved in (11) is not uniquely determined from the invertibility of $\mathbf{G}_{u,\mathbf{j}_u^{(k)}}$. Indeed, there are multiple options to select $\mathbf{W}_{u,\mathbf{j}_u^{(k)}}$, all fulfilling the condition described by (10).

A prominent choice for the whitening matrix involves Cholesky factorization [14], which leads to the following selection of

$$\mathbf{W}_{u,\mathbf{j}_u^{(k)}} = \mathbf{Q}^{-1}_{u,\mathbf{j}_u^{(k)}}, \quad \mathbf{G}_{u,\mathbf{j}_u^{(k)}} = \mathbf{Q}_{u,\mathbf{j}_u^{(k)}} \mathbf{Q}^{\intercal}_{u,\mathbf{j}_u^{(k)}}. \tag{12}$$

Here, $\mathbf{Q}_{u,\mathbf{j}_u^{(k)}}$ is a real-valued $(L_{u,|\mathbf{j}_u^{(k)}|} \times L_{u,|\mathbf{j}_u^{(k)}|})$ lower-triangular matrix determined from the Cholesky factorization of $\mathbf{G}_{u,\mathbf{j}_u^{(k)}}$. Interested readers are encouraged to review prior works [14,26] on additional choices for the whitening matrix.

The four-step algorithm described in the preceding should be repeated for all $k = 1, \dots, \bar{L}_{u,m}$. The result is a set of orthogonal polynomials

$$\left\{ \Psi_{u,\mathbf{j}_u^{(1)}}(\mathbf{x}_u), \dots, \Psi_{u,\mathbf{j}_u^{(L_{u,m})}}(\mathbf{x}_u) \right\} = \left\{ \Psi_{u,\mathbf{j}_u}(\mathbf{x}_u) : \mathbf{j}_u \in \bar{\mathcal{I}}_{u,m} \right\} \tag{13}$$

in $\mathbf{x}_u$ of degree at most m that are consistent with the probability measure $f_{\mathbf{X}_u}(\mathbf{x}_u)d\mathbf{x}_u$ of $\mathbf{X}_u$. Both forms of the polynomial set described in (13) will be used in this paper.

3.2. Statistical properties

When the input random variables are used as the argument, $\Psi_{u,\mathbf{j}_u^{(k)}}(\mathbf{X}_u)$ becomes a random polynomial in $\mathbf{X}_u$. Therefore, it is important to establish its first- and second-order moment properties, presented as follows.

3.2.1. First-order moments

Applying the expectation operator on (11), the first-order moment of the kth polynomial $\Psi_{u,\mathbf{j}_u^{(k)}}(\mathbf{X}_u)$, $k = 1, \dots, \bar{L}_{u,m}$, is

$$\begin{aligned}
\mathbb{E}\left[\Psi_{u,\mathbf{j}_u^{(k)}}(\mathbf{X}_u)\right] &= \mathbf{e}^{\intercal}_{L_{u,|\mathbf{j}_u^{(k)}|}} \mathbf{W}_{u,\mathbf{j}_u^{(k)}} \mathbb{E}\left[\mathbf{P}_{u,\mathbf{j}_u^{(k)}}(\mathbf{X}_u)\right] \\
&= \mathbf{e}^{\intercal}_{L_{u,|\mathbf{j}_u^{(k)}|}} \mathbf{Q}^{-1}_{u,\mathbf{j}_u^{(k)}} \mathbf{G}_{u,\mathbf{j}_u^{(k)}} (1,0,\dots,0)^{\intercal} \\
&= \mathbf{e}^{\intercal}_{L_{u,|\mathbf{j}_u^{(k)}|}} \mathbf{Q}^{-1}_{u,\mathbf{j}_u^{(k)}} \mathbf{Q}_{u,\mathbf{j}_u^{(k)}} \mathbf{Q}^{\intercal}_{u,\mathbf{j}_u^{(k)}} (1,0,\dots,0)^{\intercal} \\
&= \mathbf{e}^{\intercal}_{L_{u,|\mathbf{j}_u^{(k)}|}} \mathbf{Q}^{\intercal}_{u,\mathbf{j}_u^{(k)}} (1,0,\dots,0)^{\intercal} \\
&= (0,0,\dots,1)(1,0,\dots,0)^{\intercal} \\
&= 0.
\end{aligned} \tag{14}$$

Here, the second equality uses the Cholesky factorization for the whitening matrix and follows from

$$\mathbb{E}\left[\mathbf{P}_{u,\mathbf{j}_u^{(k)}}(\mathbf{X}_u)\right] = \mathbb{E}\left[\mathbf{P}_{u,\mathbf{j}_u^{(k)}}(\mathbf{X}_u)\mathbf{P}^{\intercal}_{u,\mathbf{j}_u^{(k)}}(\mathbf{X}_u)(1,0,\dots,0)^{\intercal}\right] = \mathbf{G}_{u,\mathbf{j}_u^{(k)}} (1,0,\dots,0)^{\intercal}.$$

The third equality derives from the Cholesky factorization of $\mathbf{G}_{u,\mathbf{j}_u^{(k)}}$ and the fifth equality results from the fact that $\mathbf{Q}_{u,\mathbf{j}_u^{(k)}}{}^{\intercal}$ is an upper-triangular matrix with the (1,1)th element being *one*. According to (14), the means of all non-constant orthogonal polynomials vanish for any input probability measure.

3.2.2. Second-order moments

Similarly, the second-order moment involving any two polynomials $\Psi_{u,\mathbf{j}_u^{(k)}}(\mathbf{X}_u)$ and $\Psi_{u,\mathbf{j}_u^{(l)}}(\mathbf{X}_u)$, $k,l = 1,\ldots,\bar{L}_{u,m}$ is

$$\begin{aligned}\mathbb{E}\left[\Psi_{u,\mathbf{j}_u^{(k)}}(\mathbf{X}_u)\,\Psi_{u,\mathbf{j}_u^{(l)}}(\mathbf{X}_u)\right] &= \mathbb{E}\left[\mathbf{e}^{\intercal}_{L_{u,|\mathbf{j}_u^{(k)}|}}\mathbf{W}_{u,\mathbf{j}_u^{(k)}}\mathbf{P}_{u,\mathbf{j}_u^{(k)}}(\mathbf{X}_u)\mathbf{P}_{u,\mathbf{j}_u^{(l)}}(\mathbf{X}_u)^{\intercal}\mathbf{W}^{\intercal}_{u,\mathbf{j}_u^{(l)}}\mathbf{e}_{L_{u,|\mathbf{j}_u^{(l)}|}}\right]\\ &= \mathbf{e}^{\intercal}_{L_{u,|\mathbf{j}_u^{(k)}|}}\mathbf{W}_{u,\mathbf{j}_u^{(k)}}\mathbb{E}\left[\mathbf{P}_{u,\mathbf{j}_u^{(k)}}(\mathbf{X}_u)\mathbf{P}_{u,\mathbf{j}_u^{(l)}}(\mathbf{X}_u)^{\intercal}\right]\mathbf{W}^{\intercal}_{u,\mathbf{j}_u^{(l)}}\mathbf{e}_{L_{u,|\mathbf{j}_u^{(l)}|}}.\end{aligned} \tag{15}$$

For further reduction of (15), consider the following three cases:

1. Case 1: $k = l$

$$\begin{aligned}\mathbb{E}\left[\Psi_{u,\mathbf{j}_u^{(k)}}(\mathbf{X}_u)\,\Psi_{u,\mathbf{j}_u^{(l)}}(\mathbf{X}_u)\right] &= \mathbb{E}\left[\Psi^2_{u,\mathbf{j}_u^{(k)}}(\mathbf{X}_u)\right]\\ &= \mathbf{e}^{\intercal}_{L_{u,|\mathbf{j}_u^{(k)}|}}\mathbf{W}_{u,\mathbf{j}_u^{(k)}}\mathbb{E}\left[\mathbf{P}_{u,\mathbf{j}_u^{(k)}}(\mathbf{X}_u)\mathbf{P}^{\intercal}_{u,\mathbf{j}_u^{(k)}}(\mathbf{X}_u)\right]\mathbf{W}^{\intercal}_{u,\mathbf{j}_u^{(k)}}\mathbf{e}_{L_{u,|\mathbf{j}_u^{(k)}|}}\\ &= \mathbf{e}^{\intercal}_{L_{u,|\mathbf{j}_u^{(k)}|}}\mathbf{W}_{u,\mathbf{j}_u^{(k)}}\mathbf{G}_{u,\mathbf{j}_u^{(k)}}\mathbf{W}^{\intercal}_{u,\mathbf{j}_u^{(k)}}\mathbf{e}_{L_{u,|\mathbf{j}_u^{(k)}|}}\\ &= \mathbf{e}^{\intercal}_{L_{u,|\mathbf{j}_u^{(k)}|}}\mathbf{W}_{u,\mathbf{j}_u^{(k)}}\mathbf{W}^{-1}_{u,\mathbf{j}_u^{(k)}}\mathbf{W}^{-\intercal}_{u,\mathbf{j}_u^{(k)}}\mathbf{W}^{\intercal}_{u,\mathbf{j}_u^{(k)}}\mathbf{e}_{L_{u,|\mathbf{j}_u^{(k)}|}}\\ &= \mathbf{e}^{\intercal}_{L_{u,|\mathbf{j}_u^{(k)}|}}\mathbf{I}_{L_{u,|\mathbf{j}_u^{(k)}|}}\mathbf{e}_{L_{u,|\mathbf{j}_u^{(k)}|}}\\ &= 1,\end{aligned} \tag{16}$$

   where the steps involve using a general whitening transformation matrix $\mathbf{W}_{u,\mathbf{j}_u^{(k)}}$, the definition of the monomial moment matrix $\mathbf{G}_{u,\mathbf{j}_u^{(k)}}$, and an $(L_{u,|\mathbf{j}_u^{(k)}|}\times L_{u,|\mathbf{j}_u^{(k)}|})$ identity matrix $\mathbf{I}_{L_{u,|\mathbf{j}_u^{(k)}|}}$.

2. Case 2: $k \neq l$, $|\mathbf{j}_u^{(k)}| < |\mathbf{j}_u^{(l)}|$

$$\begin{aligned}\mathbb{E}\left[\Psi_{u,\mathbf{j}_u^{(k)}}(\mathbf{X}_u)\,\Psi_{u,\mathbf{j}_u^{(l)}}(\mathbf{X}_u)\right] &= \mathbf{e}^{\intercal}_{L_{u,|\mathbf{j}_u^{(k)}|}}\mathbf{W}_{u,\mathbf{j}_u^{(k)}}\mathbb{E}\left[\bar{\mathbf{I}}_{L_{u,|\mathbf{j}_u^{(k)}|}}\mathbf{P}_{u,\mathbf{j}_u^{(l)}}(\mathbf{X}_u)\mathbf{P}^{\intercal}_{u,\mathbf{j}_u^{(l)}}(\mathbf{X}_u)\right]\mathbf{W}^{\intercal}_{u,\mathbf{j}_u^{(l)}}\mathbf{e}_{L_{u,|\mathbf{j}_u^{(l)}|}}\\ &= \mathbf{e}^{\intercal}_{L_{u,|\mathbf{j}_u^{(k)}|}}\mathbf{W}_{u,\mathbf{j}_u^{(k)}}\bar{\mathbf{I}}_{L_{u,|\mathbf{j}_u^{(k)}|}}\mathbb{E}\left[\mathbf{P}_{u,\mathbf{j}_u^{(l)}}(\mathbf{X}_u)\mathbf{P}^{\intercal}_{u,\mathbf{j}_u^{(l)}}(\mathbf{X}_u)\right]\mathbf{W}^{\intercal}_{u,\mathbf{j}_u^{(l)}}\mathbf{e}_{L_{u,|\mathbf{j}_u^{(l)}|}}\\ &= \mathbf{e}^{\intercal}_{L_{u,|\mathbf{j}_u^{(k)}|}}\mathbf{W}_{u,\mathbf{j}_u^{(k)}}\bar{\mathbf{I}}_{L_{u,|\mathbf{j}_u^{(k)}|}}\mathbf{G}_{u,\mathbf{j}_u^{(l)}}\mathbf{W}^{\intercal}_{u,\mathbf{j}_u^{(l)}}\mathbf{e}_{L_{u,|\mathbf{j}_u^{(l)}|}}\\ &= \mathbf{e}^{\intercal}_{L_{u,|\mathbf{j}_u^{(k)}|}}\mathbf{W}_{u,\mathbf{j}_u^{(k)}}\bar{\mathbf{I}}_{L_{u,|\mathbf{j}_u^{(k)}|}}\mathbf{W}^{-1}_{u,\mathbf{j}_u^{(l)}}\mathbf{W}^{-\intercal}_{u,\mathbf{j}_u^{(l)}}\mathbf{W}^{\intercal}_{u,\mathbf{j}_u^{(l)}}\mathbf{e}_{L_{u,|\mathbf{j}_u^{(l)}|}}\\ &= \mathbf{e}^{\intercal}_{L_{u,|\mathbf{j}_u^{(k)}|}}\mathbf{W}_{u,\mathbf{j}_u^{(k)}}\bar{\mathbf{I}}_{L_{u,|\mathbf{j}_u^{(k)}|}}\mathbf{W}^{-1}_{u,\mathbf{j}_u^{(l)}}\mathbf{e}_{L_{u,|\mathbf{j}_u^{(l)}|}}\\ &= \mathbf{e}^{\intercal}_{L_{u,|\mathbf{j}_u^{(k)}|}}\mathbf{W}_{u,\mathbf{j}_u^{(k)}}\mathbf{W}^{-1}_{u,\mathbf{j}_u^{(k)}}\bar{\mathbf{I}}_{L_{u,|\mathbf{j}_u^{(k)}|}}\mathbf{e}_{L_{u,|\mathbf{j}_u^{(l)}|}}\\ &= \mathbf{e}^{\intercal}_{L_{u,|\mathbf{j}_u^{(k)}|}}\bar{\mathbf{I}}_{L_{u,|\mathbf{j}_u^{(k)}|}}\mathbf{e}_{L_{u,|\mathbf{j}_u^{(l)}|}}\\ &= 0,\end{aligned} \tag{17}$$

   where the steps involve introducing an $(L_{u,|\mathbf{j}_u^{(k)}|}\times L_{u,|\mathbf{j}_u^{(l)}|})$ augmented matrix

$$\bar{\mathbf{I}}_{L_{u,|\mathbf{j}_u^{(k)}|}} = \left[\mathbf{I}_{L_{u,|\mathbf{j}_u^{(k)}|}}\middle|\mathbf{0}_{L_{u,|\mathbf{j}_u^{(k)}|}\times(L_{u,|\mathbf{j}_u^{(l)}|}-L_{u,|\mathbf{j}_u^{(k)}|})}\right],$$

   obtained by padding the identity matrix $\mathbf{I}_{L_{u,|\mathbf{j}_u^{(k)}|}}$ with *zeros* in the $(L_{u,|\mathbf{j}_u^{(k)}|}+1)$ through $L_{u,|\mathbf{j}_u^{(l)}|}$ columns of $\bar{\mathbf{I}}_{L_{u,|\mathbf{j}_u^{(k)}|}}$. In doing so, the monomial vectors $\mathbf{P}_{u,\mathbf{j}_u^{(k)}}(\mathbf{X}_u)$ and $\mathbf{P}_{u,\mathbf{j}_u^{(l)}}(\mathbf{X}_u)$ are related by

$$\mathbf{P}_{u,\mathbf{j}_u^{(k)}}(\mathbf{X}_u) = \bar{\mathbf{I}}_{L_{u,|\mathbf{j}_u^{(k)}|}}\mathbf{P}_{u,\mathbf{j}_u^{(l)}}(\mathbf{X}_u),$$

   as exploited in the first equality already. The sixth equality is formed by recognizing

$$\bar{\mathbf{I}}_{L_{u,|\mathbf{j}_u^{(k)}|}}\mathbf{W}^{-1}_{u,\mathbf{j}_u^{(l)}} = \mathbf{W}^{-1}_{u,\mathbf{j}_u^{(k)}}\bar{\mathbf{I}}_{L_{u,|\mathbf{j}_u^{(k)}|}}.$$

3. Case 3: $k \neq l$, $|\mathbf{j}_u^{(k)}| = |\mathbf{j}_u^{(l)}|$

$$\mathbb{E}\left[\Psi_{u,\mathbf{j}_u^{(k)}}(\mathbf{X}_u)\,\Psi_{u,\mathbf{j}_u^{(l)}}(\mathbf{X}_u)\right] = \int \Psi_{u,\mathbf{j}_u^{(k)}}(\mathbf{x}_u)\Psi_{u,\mathbf{j}_u^{(l)}}(\mathbf{x}_u)f_{\mathbf{X}_u}(\mathbf{x}_u)\,d\mathbf{x}_u, \tag{18}$$

   as no further reduction is possible for a general probability measure $f_{\mathbf{X}_u}(\mathbf{x}_u)\,d\mathbf{x}_u$ of $\mathbf{X}_u$.

In summary, any two polynomials in the set defined by (13) that possess distinct total degrees are mutually orthogonal with respect to any input probability measure. In contrast, two polynomials from this set that share the same total degree need not be orthogonal. This arises from the fact that, in the multivariate setting, multiple distinct polynomials may have the same total degree. Nevertheless, (13) still specifies a collection of multivariate orthogonal polynomials in $\mathbf{x}_u$ of degree at most m.

3.3. An illustrative example

Consider a UQ problem comprising $N \geq 2$ input random variables $(X_1, \ldots, X_N)^\intercal$. For $u = \{1, 2\}$, suppose the subset of input variables $(X_1, X_2)^\intercal$ comprises *zero*-mean Gaussian random variables, which have identical standard deviations $\sigma_1 = \sigma_2 = \frac{1}{4}$ and correlation coefficient $\rho = \frac{1}{5}$. Set $m = 3$ to generate at most third-order measure-consistent bivariate orthogonal polynomials in $(x_1, x_2)^\intercal$ using the four-step algorithm.

Given $u = \{1, 2\}$ and $m = 3$, the monomial set

$$\mathcal{B}_{\{1,2\},3} = \{1,\ x_1,\ x_2,\ x_1^2,\ x_1x_2,\ x_2^2,\ x_1^3,\ x_1^2x_2,\ x_1x_2^2,\ x_2^3\},$$

arranged in a graded reverse lexicographic order, is a basis of $\Pi_{\{1,2\},3}$, the vector space of polynomials in $(x_1, x_2)^\intercal$ of degree at most three. The set contains three bivariate monomials: x_1x_2, $x_1^2x_2$, and $x_1x_2^2$. Therefore, there are three bivariate orthogonal polynomials corresponding to these three monomials. Using the four-step algorithm,

$$\begin{aligned} & \left\{ \Psi_{\{1,2\}\mathbf{j}^{(1)}_{\{1,2\}}}(x_1,x_2), \Psi_{\{1,2\}\mathbf{j}^{(2)}_{\{1,2\}}}(x_1,x_2), \Psi_{\{1,2\}\mathbf{j}^{(3)}_{\{1,2\}}}(x_1,x_2) \right\} \\ = & \left\{ \Psi_{\{1,2\},(1,1)}(x_1,x_2), \Psi_{\{1,2\},(2,1)}(x_1,x_2), \Psi_{\{1,2\},(1,2)}(x_1,x_2) \right\} \\ = & \left\{ \begin{array}{c} \frac{1}{\sqrt{26}} - \frac{25}{3}\sqrt{\frac{2}{13}}x_1^2 - \frac{25}{3}\sqrt{\frac{2}{13}}x_2^2 + \frac{10}{3}\sqrt{26}x_1x_2, \\ \frac{5}{3}x_1 - 3x_2 - \frac{250}{27}x_1^3 - \frac{170}{9}x_1x_2^2 + \frac{50}{27}x_2^3 + 50x_1^2x_2, \\ -3x_1 + \frac{5}{3}x_2 + \frac{50}{27}x_1^3 - \frac{170}{9}x_1^2x_2 - \frac{250}{27}x_2^3 + 50x_1x_2^2 \end{array} \right\} \end{aligned} \tag{19}$$

is the set of such orthogonal polynomials in $(x_1, x_2)^\intercal$ of degree at most three. Appendix A provides further details on the steps of the algorithm, producing these orthogonal polynomials.

It is straightforward to verify that the polynomials in (19) satisfy the statistical properties specified in (14), (16), and (17). It should be emphasized, however, that these closed-form expressions are attainable primarily because, under a Gaussian probability measure, the moment matrix and its Cholesky factorization can be constructed analytically and hence exactly. For general probability distributions, deriving measure-consistent orthogonal polynomials analytically is seldom feasible. In such cases, approximate or numerical procedures must be employed to build the moment matrix, resulting in approximate orthogonal polynomials, as will be further elucidated in Section 5.

3.4. A few remarks

The effectiveness of the four-step algorithm for generating orthogonal polynomials depends critically on a well-conditioned moment matrix $\mathbf{G}_{u\mathbf{j}_u^{(k)}}$, which is necessary for successful Cholesky factorization. However, as the polynomial order m increases, the condition number of $\mathbf{G}_{u\mathbf{j}_u^{(k)}}$ grows rapidly with increasing $|\mathbf{j}_u^{(k)}| \leq m$, potentially causing numerical instability [27]. In practice, though, the polynomial order m is typically confined to a modest range – commonly between one and four – within which Cholesky factorization of the moment matrix can generally be performed without significant computational difficulty.

A fundamental distinction between univariate and multivariate orthogonal polynomials is the lack of a unique, natural ordering for the latter. In the univariate case, monomials are naturally ordered by their degree. In contrast, multivariate polynomials can be arranged according to various schemes, including lexicographic order, graded lexicographic order, and graded reverse lexicographic order, among others. No single ordering is intrinsically better, and the choice of ordering directly affects the resulting sequence of orthogonal polynomials.

4. Generalized polynomial dimensional decomposition

The GPDD of an output random variable $y(\mathbf{X}) \in L^2(\Omega, \mathcal{F}, \mathbb{P})$ is an infinite series expansion of $y(\mathbf{X})$ with respect to a complete, hierarchically ordered, orthogonal polynomial basis of $L^2(\Omega, \mathcal{F}, \mathbb{P})$. The expansion, derived from a generalized analysis-of-variance (ANOVA) dimensional decomposition (ADD) [28], is briefly outlined here. For a more rigorous treatment involving dimensionwise splitting of polynomial spaces and functional-analytic considerations, readers should consult the foundation works on GPDD [15,16].

4.1. Generalized ADD

Under Assumption 1, a square-integrable function $y(\mathbf{X}) \in L^2(\Omega, \mathcal{F}, \mathbb{P})$ of input variables $\mathbf{X}$ admits a unique, finite, hierarchical expansion [28]

$$y(\mathbf{X}) = y_\emptyset + \sum_{\emptyset \neq u \subseteq \{1,\ldots,N\}} y_u(\mathbf{X}_u), \tag{20a}$$

$$y_\emptyset = \int_{\mathbb{A}^N} y(\mathbf{x}) f_{\mathbf{X}}(\mathbf{x}) d\mathbf{x}, \tag{20b}$$

$$y_u(\mathbf{X}_u) = \int_{\mathbb{A}^{-u}} y(\mathbf{X}_u, \mathbf{x}_{-u}) f_{\mathbf{X}_{-u}}(\mathbf{x}_{-u}) d\mathbf{x}_{-u} - \sum_{v \subset u} y_v(\mathbf{X}_v) - \sum_{\substack{\emptyset \neq v \subseteq \{1,\dots,N\} \\ v \cap u \neq \emptyset, v \nsubseteq u}} \int_{\mathbb{A}^{v \cap -u}} y_v(\mathbf{X}_{v \cap u}, \mathbf{x}_{v \cap -u}) f_{\mathbf{X}_{v \cap -u}}(\mathbf{x}_{v \cap -u}) d\mathbf{x}_{v \cap -u}, \tag{20c}$$

in terms of its input variables with increasing dimensions, where $u \subseteq \{1, \dots, N\}$ is a subset with the complementary set $-u = \{1, \dots, N\} \backslash u$ and y_u is a $|u|$-variate component function describing a constant or an $|u|$-variate interaction of $\mathbf{X}_u = (X_{i_1}, \dots, X_{i_{|u|}})$ on y when $|u| = 0$ or $|u| > 0$. This expansion is known as the generalized ADD [28]. Although it was originally derived using $\mathbb{A}^N = \mathbb{R}^N$ [28], the extension for the case of $\mathbb{A}^N \subseteq \mathbb{R}^N$ is trivial. Here, $(\mathbf{X}_u, \mathbf{x}_{-u})$ denotes an N-dimensional vector whose ith component is X_i if $i \in u$ and x_i if $i \notin u$. Similar to the classical ADD, the summation in (20a) comprises $2^N - 1$ terms with each term depending on a group of variables indexed by a particular subset of $\{1, \dots, N\}$. When $u = \emptyset$, both sums in (20c) vanish, resulting in the expression of the constant function $y_\emptyset$ in (20b). When $u = \{1, \dots, N\}$, the integration in the first line of (20c) is on the empty set and the sum in the second line of (20c) vanishes, reproducing (20a) and hence finding the last function $y_{\{1,\dots,N\}}$. Indeed, all component functions of y can be obtained by interpreting literally (20c).

The generalized ADD described by (20a)-(20c) has two notable properties [28,29]:

1. The component functions y_u, where $\emptyset \neq u \subseteq \{1, \dots, N\}$, have zero means, that is,

$$\mathbb{E}\left[y_u(\mathbf{X}_u)\right] = 0; \tag{21}$$

and

2. Two distinct component functions y_u and y_v, where $\emptyset \neq u \subseteq \{1, \dots, N\}$, $\emptyset \neq v \subseteq \{1, \dots, N\}$, and $v \subset u$, are hierarchically orthogonal, that is, they satisfy the property

$$\mathbb{E}\left[y_u(\mathbf{X}_u) y_v(\mathbf{X}_v)\right] = 0. \tag{22}$$

Further details of the generalized ADD are available in a previous work of the authors [28].

4.2. Generalized PDD

The GPDD of a random variable $y(\mathbf{X}) \in L^2(\Omega, \mathcal{F}, \mathbb{P})$ is obtained when all non-constant component functions $y_u(\mathbf{X}_u)$, $u \subseteq \{1, \dots, N\}$, of the generalized ADD are expanded with respect to a complete set of measure-consistent orthogonal polynomials in $\mathbf{X}_u$.

Theorem 1 ([15,16]). *Let $\mathbf{X} := (X_1, \dots, X_N)^T$ be a vector of $N \in \mathbb{N}$ input random variables fulfilling Assumption 1. For $\emptyset \neq u \subseteq \{1, \dots, N\}$ and $\mathbf{X}_u := (X_{i_1}, \dots, X_{i_{|u|}})^T : (\Omega^u, \mathcal{F}^u) \to (\mathbb{A}^u, \mathcal{B}^u)$, denote by $\{\Psi_{u,\mathbf{j}_u}(\mathbf{x}_u) : \mathbf{j}_u \in \mathbb{N}^{|u|}\}$ the set of multivariate orthogonal polynomials consistent with the probability measure $f_{\mathbf{X}_u}(\mathbf{x}_u) d\mathbf{x}_u$. Then, for any random variable $y(\mathbf{X}) \in L^2(\Omega, \mathcal{F}, \mathbb{P})$, there exists a Fourier-like series in multivariate orthogonal polynomials in $\mathbf{X}_u$, referred to as the GPDD of*

$$y(\mathbf{X}) \sim y_\emptyset + \sum_{\emptyset \neq u \subseteq \{1,\dots,N\}} \sum_{\mathbf{j}_u \in \mathbb{N}^{|u|}} C_{u,\mathbf{j}_u} \Psi_{u,\mathbf{j}_u}(\mathbf{X}_u), \tag{23}$$

where the zero-variate, expansion coefficient $y_\emptyset \in \mathbb{R}$ is defined by

$$y_\emptyset := \mathbb{E}[y(\mathbf{X})] := \int_{\mathbb{A}^N} y(\mathbf{x}) f_{\mathbf{X}}(\mathbf{x}) d\mathbf{x} \tag{24}$$

and the $|u|$-variate, $|\mathbf{j}_u|$th-order expansion coefficients $C_{u,\mathbf{j}_u} \in \mathbb{R}$ satisfy the infinite-dimensional linear system

$$\sum_{\emptyset \neq v \subseteq \{1,\dots,N\}} \sum_{\mathbf{k}_v \in \mathbb{N}^{|v|}} C_{v,\mathbf{k}_v} J_{u,\mathbf{j}_u;v,\mathbf{k}_v} = I_{u,\mathbf{j}_u}, \ \emptyset \neq u \subseteq \{1, \dots, N\}, \ \mathbf{j}_u \in \mathbb{N}^{|u|}, \tag{25}$$

with the integrals

$$I_{u,\mathbf{j}_u} := \mathbb{E}\left[y(\mathbf{X}) \Psi_{u,\mathbf{j}_u}(\mathbf{X}_u)\right] := \int_{\mathbb{A}^N} y(\mathbf{x}) \Psi_{u,\mathbf{j}_u}(\mathbf{x}_u) f_{\mathbf{X}}(\mathbf{x}) d\mathbf{x}, \tag{26a}$$

$$J_{u,\mathbf{j}_u;v,\mathbf{k}_v} := \mathbb{E}\left[\Psi_{u,\mathbf{j}_u}(\mathbf{X}_u) \Psi_{v,\mathbf{k}_v}(\mathbf{X}_v)\right] := \int_{\mathbb{A}^N} \Psi_{u,\mathbf{j}_u}(\mathbf{x}_u) \Psi_{v,\mathbf{k}_v}(\mathbf{x}_v) f_{\mathbf{X}}(\mathbf{x}) d\mathbf{x}. \tag{26b}$$

Furthermore, the GPDD of $y(\mathbf{X}) \in L^2(\Omega, \mathcal{F}, \mathbb{P})$ converges to $y(\mathbf{X})$ in mean-square, in probability, and in distribution. Here, the symbol $\sim$ in (23) represents equality in a weaker sense, such as equality in mean-square, but not necessarily pointwise nor almost everywhere.

The proof is omitted here, as it is available elsewhere [15,16].

4.3. GPDD Approximation

The full GPDD contains an infinite number of orthogonal polynomials or coefficients. In practice, however, the expansion must be truncated to a finite number of terms. Several truncation strategies exist. In this work, a straightforward approach is adopted, consisting of (1) retaining all polynomials involving at most $0 \le S \le N$ variables, thereby limiting the degree of interaction among input variables to S, and (2) preserving polynomial expansion orders or total degree less than or equal to $S \le m < \infty$. The resulting truncation is referred to as an S-variate, mth-order GPDD approximation[2]

$$y_{S,m}(\mathbf{X}) = y_{\emptyset} + \sum_{\substack{\emptyset \neq u \subseteq \{1,\dots,N\} \\ 1 \le |u| \le S}} \sum_{\substack{\mathbf{j}_u \in \mathbb{N}^{|u|} \\ |u| \le |\mathbf{j}_u| \le m}} C_{u,\mathbf{j}_u} \Psi_{u,\mathbf{j}_u}(\mathbf{X}_u) \tag{27}$$

of $y(\mathbf{X})$, comprising

$$L_{S,m} = 1 + \sum_{s=1}^{S} \binom{N}{s} \binom{m}{s}, \tag{28}$$

number of basis functions or expansion coefficients.

Several clarifications regarding the truncated GPDD are in order. First, the truncation with respect to the expansion order in (27) is based on the total-degree index set. Alternative truncation schemes, such as tensor-product or hyperbolic-cross index sets, are not considered in this work. Second, the right-hand side of (27) contains sums of at most S-variate orthogonal polynomials. Accordingly, the term "S-variate" in describing the GPDD approximation should be understood as indicating the inclusion of interactions among at most S input variables, even though $y_{S,m}$ itself remains an N-variate function. Finally, in the limit, when $S \to N$ and $m \to \infty$, the approximation $y_{S,m}$ converges to y in the mean-square sense, generating a hierarchical and convergent sequence of GPDD approximations.

The motivation for generalized ADD- and GPDD-derived approximations is as follows. In practical applications, the function $y(\mathbf{X})$ often exhibits an effective dimension [30] that is much smaller than N, implying that the right side of (20a) can be accurately represented by a sum of lower-dimensional component functions y_u with $|u| \ll N$, while still incorporating all random variables $\mathbf{X}$ in a high-dimensional UQ problem. For instance, an S-variate, mth-order GPDD approximation $y_{S,m}(\mathbf{X})$ can be constructed, where $0 \le S \le N$ and $S \le m < \infty$ specify the maximum degree of interactions among input variables and the highest polynomial order retained in the corresponding truncation. This approximation is based on a widely observed property in real-world problems: for a high-dimensional function y, the $|u|$-variate, $|\mathbf{j}_u|$th-order GPDD component function $C_{u,\mathbf{j}_u}\Psi_{u,\mathbf{j}_u}(\mathbf{X}_u)$ typically decays rapidly as $|u|$ and $|\mathbf{j}_u|$ increase, enabling accurate low-variate, low-order approximation of y.

4.4. Second-moment analysis

The S-variate, mth-order GPDD approximation $y_{S,m}(\mathbf{X})$ can be regarded as a computationally inexpensive surrogate for the original, potentially expensive-to-evaluate function $y(\mathbf{X})$. Consequently, key statistical properties of $y(\mathbf{X})$, such as its first and second moments, can be accurately estimated using the corresponding moments of $y_{S,m}(\mathbf{X})$.

Applying the expectation operator on $y_{S,m}(\mathbf{X})$ in (27) and recognizing (14), its mean

$$\mathbb{E}\big[y_{S,m}(\mathbf{X})\big] = \mathbb{E}[y(\mathbf{X})] = y_{\emptyset} \tag{29}$$

matches the exact mean of $y(\mathbf{X})$ for any $0 \le S \le N$ and $m \in \mathbb{N}_0$. Enforcing the expectation operator again, this time on $(y_{S,m}(\mathbf{X}) - \mathbb{E}[y_{S,m}(\mathbf{X})])^2$, results in the variance

$$\mathrm{var}\big[y_{S,m}(\mathbf{X})\big] = \sum_{\substack{\emptyset \neq u,v \subseteq \{1,\dots,N\} \\ 1 \le |u| \le S \\ 1 \le |v| \le S}} \sum_{\substack{\mathbf{j}_u \in \mathbb{N}^{|u|}, \mathbf{k}_v \in \mathbb{N}^{|v|} \\ |u| \le |\mathbf{j}_u| \le m \\ |v| \le |\mathbf{k}_v| \le m}} C_{u,\mathbf{j}_u} C_{v,\mathbf{k}_v} J_{u,\mathbf{j}_u;v,\mathbf{k}_v} \tag{30}$$

of $y_{S,m}(\mathbf{X})$. Here, according to (16) and (17), many of the integrals $J_{u,\mathbf{j}_u;v,\mathbf{k}_v}$ vanish or become equal to *one*, depending on u, v, $\mathbf{j}_u$ and $\mathbf{k}_v$. It is elementary to show that the variance of the truncated GPDD converges to the variance of GPDD when $S \to N$ and $m \to \infty$. Therefore, the second-moment statistics of a GPDD approximation are solely determined by an appropriately truncated set of expansion coefficients and statistical properties of random orthogonal polynomials.

4.5. Reliability analysis

A fundamental problem in reliability analysis entails calculation of the failure probability

$$P_F := \mathbb{P}[\mathbf{X} \in \Omega_F] = \int_{\mathbb{A}^N} I_{\Omega_F}(\mathbf{x}) f_{\mathbf{X}}(\mathbf{x}) d\mathbf{x} =: \mathbb{E}\Big[I_{\Omega_F}(\mathbf{X})\Big], \tag{31}$$

where $I_{\Omega_F}(\mathbf{x})$ is the indicator function associated with the failure domain Ω_F, which is equal to *one* when $\mathbf{x} \in \Omega_F$ and *zero* otherwise. For a component reliability analysis, the failure domain is often adequately described by a single performance function $y(\mathbf{X})$, for

[2] The nouns *degree* and *order* associated with GPDD or orthogonal polynomials are used synonymously in the paper.

instance, $\Omega_F := \{\mathbf{x} : y(\mathbf{x}) < 0\}$, whereas multiple, interdependent performance functions are required for a system reliability analysis. In this work, only component reliability analysis is considered.

If the function $y(\mathbf{X})$ is sufficiently smooth, its S-variate, mth-order GPCE approximation $y_{S,m}(\mathbf{X})$ may potentially be used for reliability analysis too. In this regard, let $\Omega_{F,S,m} := \{\mathbf{x} : y_{S,m}(\mathbf{x}) < 0\}$ be an approximate failure set. Then, an estimate of the failure probability P_F in (31), obtained using MCS of the GPDD approximation, is

$$P_{F,S,m} = \mathbb{E}\left[I_{\Omega_{F,S,m}}(\mathbf{X})\right] = \lim_{L'\to\infty} \frac{1}{L'} \sum_{l=1}^{L'} I_{\Omega_{F,S,m}}(\mathbf{x}^{(l)}), \tag{32}$$

where L' is the sample size of the GPDD approximation, $\mathbf{x}^{(l)}$ is the lth realization of $\mathbf{X}$, and $I_{\Omega_{F,S,m}}(\mathbf{x})$ is another indicator function, which is equal to *one* when $\mathbf{x} \in \Omega_{F,S,m}$ and *zero* otherwise.

It should be emphasized that the simulation of the GPDD approximation in (32) is fundamentally different from crude MCS typically used for producing benchmark results. A crude MCS requires direct numerical evaluation of $y(\mathbf{x}^{(l)})$ for input samples $\mathbf{x}^{(l)}$, $l = 1, \ldots, L_{MCS}$, with $L_{MCS} \in \mathbb{N}$. Such calculations can be computationally expensive or even prohibitive, especially when a very large sample size is required to estimate small failure probabilities. In contrast, MCS of the GPDD approximation involves only evaluations of simple polynomial functions describing $y_{S,m}(\mathbf{x}^{(l)})$. Therefore, a relatively large sample size (L') can be accommodated in the GPDD approximation even when y is expensive to evaluate.

4.6. Comparison with GPCE

While GPDD emphasizes a dimensionwise, Fourier-like expansion in orthogonal polynomials, it is instructive to compare it with alternative expansions, such as GPCE [14,31], which also employ orthogonal polynomials but without a hierarchical, dimensionwise structure. Two notable observations emerge from this comparison.

First, GPDD operates using low-variate marginal distributions, thereby avoiding the need for the full joint distribution of a high-dimensional random input. As a result, a GPDD approximation involves only low-variate multivariate polynomials, in contrast to the high-variate polynomials required in a GPCE approximation. Consequently, the computational effort to construct the polynomial basis in GPDD is generally lower than in GPCE. Moreover, in practical scenarios where the joint distribution is unknown and only marginal distributions are available, GPDD can still be applied by generating measure-consistent multivariate polynomials over subsets of input variables.

Second, in UQ problems where the output function is highly nonlinear but the interactions among input variables are relatively weak – a situation commonly observed in practical applications – the GPDD approximation is expected to offer significantly greater computational efficiency than the GPCE approximation. This efficiency stems from GPDD's dimensionwise, hierarchical structure, which allows the approximation to exploit low-variate interactions, a feature not shared by GPCE.

5. Practical GPDD approximation

The GPDD approximation presented in Section 4 constitutes a theoretical formulation. In practice, this formulation is not directly implementable because, for a general UQ problem with an arbitrary output function and an arbitrary input probability distribution, neither the orthogonal polynomial basis nor the corresponding expansion coefficients can be determined exactly. In this section, a computationally tractable GPDD approximation is developed, emphasizing its suitability for real-world applications.

5.1. Generation of approximate orthogonal polynomials

For a random input $\mathbf{X}$ following an arbitrary probability measure $f_{\mathbf{X}}(\mathbf{x})d\mathbf{x}$, the expectations $G_{u,\mathbf{j}_u^{(k)},pq}$ in (9), which generally involve multidimensional integration, cannot be computed analytically or exactly. Consequently, only its estimate, denoted by $\tilde{G}_{u,\mathbf{j}_u^{(k)},pq}$, leading to approximate monomial moment matrix $\tilde{\mathbf{G}}_{u,\mathbf{j}_u^{(k)}}$ (say) can be attained in a practical setting. Various techniques, including numerical integration or sampling-based methods, may be employed for the approximation. In this work, the authors propose a Gauss quadrature rule in tandem with a measure transformation to calculate $\tilde{G}_{u,\mathbf{j}_u^{(k)},pq}$, as follows.

For a given $\emptyset \neq u \subset \{1, \ldots, N\}$, consider a change of variables from $\mathbf{x}_u = (x_{i_1}, \ldots, x_{i_{|u|}})$ to $\mathbf{z}_u = (z_{i_1}, \ldots, z_{i_{|u|}})$ (say), where z_{i_l}, $l = 1, \ldots, |u|$, is a realization of a continuous independent random variable Z_{i_l}, which has absolutely continuous CDF $F_{Z_{i_l}}(z_{i_l}) := \mathbb{P}[Z_{i_l} \leq z_{i_l}]$ and continuous PDF $f_{Z_{i_l}}(z_{i_l}) := dF_{Z_{i_l}}(z_{i_l})/dz_{i_l}$ supported on a bounded or an unbounded interval $[a_{i_l}, b_{i_l}] \subseteq \mathbb{R}$, $a_{i_l}, b_{i_l} \in \mathbb{R}$, $b_{i_l} > a_{i_l}$. For instance, the change of variables from the commonly used Rosenblatt transformation [11] is

$$\begin{aligned} x_{i_1} &= F^{-1}_{X_{i_1}}[F_{Z_{i_1}}(z_{i_1})] \\ x_{i_2} &= F^{-1}_{X_{i_2}|X_{i_1}}[F_{Z_{i_2}}(z_{i_2})|x_{i_1}] \\ &\vdots \\ x_{i_{|u|}} &= F^{-1}_{X_{i_{|u|}}|X_{i_1},\ldots,X_{i_{|u|-1}}}[F_{Z_{i_{|u|}}}(z_{i_{|u|}})|x_{i_1}, \ldots, x_{i_{|u|-1}}], \end{aligned} \tag{33}$$

where $F_{X_{i_1}}(x_{i_1}) := \mathbb{P}[X_{i_1} \le x_{i_1}]$ is the marginal CDF of X_{i_1} and

$$F_{X_{i_l}|X_{i_1},\dots,X_{i_{l-1}}}(x_{i_l}) := \mathbb{P}[X_{i_l} \le x_{i_l} | X_{i_1} = x_{i_1}, \dots, X_{i_{l-1}} = x_{i_{l-1}}],\ l = 2, \dots, |u|,$$

is a conditional CDF of X_{i_l}. Then, using (33) in (9), the expectation becomes

$$\begin{aligned} \tilde{G}_{u,\mathbf{j}_u^{(k)},pq} &:= \int_{\mathbb{A}^u} x_{i_1}^{j_{i_1}^{(p)}+j_{i_1}^{(q)}} \cdots x_{i_{|u|}}^{j_{i_{|u|}}^{(p)}+j_{i_{|u|}}^{(q)}} f_{\mathbf{X}_u}(\mathbf{x}_u) d\mathbf{x}_u \\ &= \int_{\times_{l=1}^{|u|}[a_{i_l},b_{i_l}]} x_{i_1}^{j_{i_1}^{(p)}+j_{i_1}^{(q)}} \cdots x_{i_{|u|}}^{j_{i_{|u|}}^{(p)}+j_{i_{|u|}}^{(q)}} \frac{f_{Z_{i_1}}(z_{i_1}) \cdots f_{Z_{i_{|u|}}}(z_{i_{|u|}})}{f_{\mathbf{X}_u(\mathbf{x}_u)}} f_{\mathbf{X}_u}(\mathbf{x}_u) d\mathbf{z}_u \\ &= \int_{\times_{l=1}^{|u|}[a_{i_l},b_{i_l}]} x_{i_1}^{j_{i_1}^{(p)}+j_{i_1}^{(q)}} \cdots x_{i_{|u|}}^{j_{i_{|u|}}^{(p)}+j_{i_{|u|}}^{(q)}} f_{Z_{i_1}}(z_{i_1}) \cdots f_{Z_{i_{|u|}}}(z_{i_{|u|}}) dz_{i_1} \cdots dz_{i_{|u|}}. \end{aligned} \tag{34}$$

Here, in the second line the quotient in the integrand is the determinant of the Jacobian of the transformation and the monomial in the integrand is a function of $\mathbf{z}_u$, as described in (33). Compared with (9), which represents a $|u|$-dimensional integral on a possibly non-rectangular domain $\mathbb{A}^u$, the last line of (34) is a $|u|$-dimensional integral on a rectangular domain $\times_{l=1}^{|u|}[a_{i_l}, b_{i_l}]$ with a separable PDF as the kernel. Still, an analytic evaluation of the integral is impossible for a general probability measure of $\mathbf{X}_u$, suggesting a need for further numerical approximation. Henceforth, a general anisotropic $(n_{i_1}, \dots, n_{i_{|u|}})$-point, multivariate, tensor-product Gauss-type quadrature rule yields an estimate

$$\tilde{G}_{u,\mathbf{j}_u^{(k)},pq} \simeq \underbrace{\sum_{r_{i_1}=1}^{n_{i_1}} \cdots \sum_{r_{i_{|u|}}=1}^{n_{|u|}}}_{|u| \text{ sums}} \left(x_{i_1}^{(r_{i_1})}\right)^{j_{i_1}^{(p)}+j_{i_1}^{(q)}} \cdots \left(x_{i_{|u|}}^{(r_{i_{|u|}})}\right)^{j_{i_{|u|}}^{(p)}+j_{i_{|u|}}^{(q)}} \prod_{l=1}^{|u|} w_{i_l}^{(r_{i_l})}, \tag{35}$$

of $G_{u,\mathbf{j}_u^{(k)},pq}$, where

$$x_{i_l}^{(r_{i_l})} = \begin{cases} F_{X_{i_1}}^{-1}[F_{Z_{i_1}}(z_{i_1}^{(r_{i_1})})], & l = 1, \\ F_{X_{i_l}|X_{i_1},\dots,X_{i_{l-1}}}^{-1}[F_{Z_{i_l}}(z_{i_l}^{(r_{i_l})}) | x_{i_1}^{(r_{i_1})}, \dots, x_{i_{l-1}}^{(r_{i_{l-1}})}], & l = 2, \dots, |u|, \end{cases}$$

and, for each $l = 1, \dots, |u|$, $z_{i_l}^{(r_{i_l})}$ and $w_{i_l}^{(r_{i_l})}$ are integration points and matching weights, respectively, with r_{i_l} running from 1 to $n_{i_l} \in \mathbb{N}$. The integration points and associated weights depend on the probability measure $f_{Z_{i_l}}(z_{i_l})dz_{i_l}$ of Z_{i_l} and are readily available from existing methods, such as the Stieltjes procedure [32,33], to generate the measure-consistent Gauss quadrature formulae. If the PDFs of Z_{i_l} are identical and $n_{i_1} = \cdots = n_{i_{|u|}} = n$ (say), then the result is an n-point isotropic quadrature rule. Note that the Rosenblatt transformation, used here solely for constructing the moment matrix, should not be confused with the form typically applied to map output functions in the presence of dependent variables.

Replacing $\mathbf{G}_{u,\mathbf{j}_u^{(k)}}$ with $\tilde{\mathbf{G}}_{u,\mathbf{j}_u^{(k)}}$, where all components of the latter are obtained using the aforementioned Gauss quadrature rule, the four-step algorithm described in Section 3 produces an approximate version of the mth-order orthogonal polynomial basis in $\mathbf{x}_u$. Denote by

$$\left\{\tilde{\Psi}_{u,\mathbf{j}_u^{(1)}}(\mathbf{x}_u), \dots, \tilde{\Psi}_{u,\mathbf{j}_u^{(\bar{L}_{u,m})}}(\mathbf{x}_u)\right\} = \left\{\tilde{\Psi}_{u,\mathbf{j}_u}(\mathbf{x}_u) : |u| \le \mathbf{j}_u \le m\right\}$$

the set of such approximate polynomials in $\mathbf{x}_u$ of degree at most m that are consistent with the probability measure $f_{\mathbf{X}_u}(\mathbf{x}_u)d\mathbf{x}_u$ of $\mathbf{X}_u$. The total number of polynomials is still $\bar{L}_{u,m}$.

For an S-variate, mth-order GPDD approximation, the aforementioned polynomial set should be constructed for all $0 \le |u| \le S$ and $|u| \le \mathbf{j}_u \le m$. As a result, the total number of orthogonal polynomial basis functions in an S-variate, mth-order GPDD approximation is $L_{S,m}$, as determined by (28).

5.2. Estimation of expansion coefficients

According to (24) through (26), the evaluation of the expansion coefficients $y_\emptyset$ and $C_{u,\mathbf{j}_u}$, $1 \le |u| \le S$, $|u| \le \mathbf{j}_u \le m$, of an S-variate, mth-order GPDD approximation $y_{S,m}(\mathbf{X})$ requires the computation of various high-dimensional integrals. For a general output function y and/or an arbitrary probability distribution of random input $\mathbf{X}$, exact evaluation of these coefficients from the definitions alone is infeasible. Numerical integration entailing a multivariate Gauss-type quadrature rule is computationally formidable and likely prohibitive when the function evaluations are expensive and the stochastic dimension N exceeds four or five. In this context, a practical alternative is to employ standard least-squares (SLS) regression, in which a pre-determined input-output data set is fitted to estimate the coefficients, as follows.

While the compact notations used in (27) enable a concise description of GPDD, a version using a single index notation is better suited for calculating the GPDD coefficients. In this case, organize the elements of the sets of approximate GPDD basis and coefficients

$$\{\tilde{\Psi}_{u,\mathbf{j}_u}(\mathbf{X}_u) : 0 \le |u| \le S, |u| \le \mathbf{j}_u \le m\} \text{ and } \{\tilde{C}_{u,\mathbf{j}_u} : 0 \le |u| \le S, |u| \le \mathbf{j}_u \le m\}$$

as

$$\{\tilde{\Psi}_1(\mathbf{X}), \dots, \tilde{\Psi}_{L_{S,m}}(\mathbf{X})\} \text{ and } \{\tilde{C}_1, \dots, \tilde{C}_{L_{S,m}}\},$$

respectively. As a result, the S-variate, mth-order GPDD approximation using approximate basis, denoted by $\tilde{y}_{S,m}(\mathbf{X})$, can also be written as

$$\tilde{y}_{S,m}(\mathbf{X}) = \sum_{i=1}^{L_{S,m}} \tilde{C}_i \tilde{\Psi}_i(\mathbf{X}). \tag{36}$$

From the known probability distribution of random input $\mathbf{X}$ and an output function $y : \mathbb{A}^N \to \mathbb{R}$, consider a deterministic input-output data set

$$\left\{\mathbf{x}^{(l)}, y(\mathbf{x}^{(l)})\right\}_{l=1}^{L}$$

of size $L \in \mathbb{N}$. The mapping y may range from a simple, explicitly defined mathematical function to a complex, implicitly defined function obtained through computational simulations, such as finite-element analysis (FEA) of a complex mechanical system. In either case, the data set, often referred to as the experimental design, can be generated by calculating the function $y(\mathbf{x}^{(l)})$ at each input sample $\mathbf{x}^{(l)}$. Various sampling strategies, namely, standard MCS, quasi MCS, and Latin hypercube sampling, can be used to build the experimental design.

According to SLS, the expansion coefficients are estimated by minimizing the empirical analog of the mean-squared error

$$\frac{1}{L}\sum_{l=1}^{L}\left[y(\mathbf{x}^{(l)}) - \sum_{i=1}^{L_{S,m}} C_i \tilde{\Psi}_i(\mathbf{x}^{(l)})\right]^2, \; C_i \in \mathbb{R}, \tag{37}$$

committed by the GPDD approximation $\tilde{y}_{S,m}(\mathbf{X})$ of $y(\mathbf{X})$. The resultant SLS solution of the expansion coefficients, denoted by

$$\tilde{\mathbf{c}} := \left(\tilde{C}_1, \dots, \tilde{C}_{L_{S,m}}\right)^\intercal,$$

is obtained from

$$\mathbf{A}^\intercal\mathbf{A}\tilde{\mathbf{c}} = \mathbf{A}^\intercal\mathbf{b}, \tag{38}$$

where

$$\mathbf{A} := \begin{bmatrix} \tilde{\Psi}_1(\mathbf{x}^{(1)} & \cdots & \tilde{\Psi}_{L_{S,m}}(\mathbf{x}^{(1)}) \\ \vdots & \ddots & \vdots \\ \tilde{\Psi}_1(\mathbf{x}^{(L)} & \cdots & \tilde{\Psi}_{L_{S,m}}(\mathbf{x}^{(L)}) \end{bmatrix}$$

is often referred to as the information or data matrix and

$$\mathbf{b} := \left(y(\mathbf{x}^{(1)}), \dots, y(\mathbf{x}^{(L)})\right)^\intercal.$$

A necessary condition for the SLS solution is the data size $L > L_{S,m}$. Even when the condition is met, the experimental design must be judiciously selected to ensure that the matrix $\mathbf{A}^\intercal\mathbf{A}$ remains well-conditioned.

5.3. Implementable GPDD approximation

Owing to the construction of the monomial moment matrix via numerical integration, the resulting whitening matrix described in Section 3 is only approximate. Consequently, the resulting orthogonal polynomials are also approximate, denoted by $\tilde{\Psi}_i(\mathbf{x})$, $i = 1, \dots, L_{S,m}$. In addition, the expansion coefficients $\tilde{C}_i$, $i = 1, \dots, L_{S,m}$, obtained using the regression procedure outlined earlier are also approximate. Therefore, instead of (27), an actual S-variate, mth-order GPDD approximation takes the form

$$\tilde{y}_{S,m}(\mathbf{X}) = \sum_{i=1}^{L_{S,m}} \tilde{C}_i \tilde{\Psi}_i(\mathbf{X}), \tag{39}$$

which is ready to be implemented for a general UQ problem.

Henceforth, the mean and variances of $\tilde{y}_{S,m}(\mathbf{X})$ are calculated from the estimated expansion coefficients as

$$\mathbb{E}[\tilde{y}_{S,m}(\mathbf{X})] \approx \tilde{C}_1 \tag{40}$$

and

$$\mathrm{var}[\tilde{y}_m(\mathbf{X})] \approx \sum_{i=2}^{L_{S,m}}\sum_{j=2}^{L_{S,m}} \tilde{C}_i\tilde{C}_j\tilde{J}_{ij}, \tag{41}$$

respectively, where

$$\tilde{J}_{ij} := \mathbb{E}\left[\tilde{\Psi}_i(\mathbf{X})\tilde{\Psi}_j(\mathbf{X})\right].$$

Again, depending on i and j, many of the integrals $\tilde{J}_{ij}$ approximately vanish or become equal to *one*, as per (16) and (17).

Similarly, for reliability analysis, the approximate failure probability is determined from

$$\tilde{P}_{F,m} = \mathbb{E}\left[I_{\tilde{\Omega}_{F,m}}(\mathbf{X})\right] = \lim_{L'\to\infty} \frac{1}{L'} \sum_{l=1}^{L'} I_{\tilde{\Omega}_{F,m}}(\mathbf{x}^{(l)}), \tag{42}$$

where $\tilde{\Omega}_{F,m} := \{\mathbf{x} : \tilde{y}_{S,m}(\mathbf{x}) < 0\}$ is the approximate failure set as a result of an S-variate, mth-order actual GPDD approximation $\tilde{y}_{S,m}(\mathbf{X})$. All numerical results of second-moment statistics and reliability analysis reported in the paper are based on the actual GPDD approximation and formulae described in (39) through (42).

5.4. Computational cost and flow

For computationally expensive models, the primary cost for creating an S-variate, mth-order GPDD approximation arises from the construction of the experimental design, producing the input-output data set $\{\mathbf{x}^{(l)}, y(\mathbf{x}^{(l)})\}_{l=1}^{L}$ of size $L \in \mathbb{N}$. When the computational effort for evaluating the output function is independent of the input data – as is commonly the case in modeling and simulation of mechanical systems – the total cost scales directly with the data size L. In SLS regression, L is typically several times larger than the number of basis functions $L_{S,m}$ to ensure the invertibility of the data matrix in (38). Because the number of GPDD basis functions increases with both S and m, minimizing L relative to $L_{S,m}$ is a critical practical consideration. The computational efficiency of the GPDD approximation will be further illustrated in the Examples and Application sections.

Fig. 1 presents the general computational flow for constructing a practical GPDD approximation. It also illustrates the subsequent evaluation of the second-moment properties and reliability for general stochastic responses.

6. Numerical examples

Three numerical examples, each designed to address a specific objective, are presented to demonstrate the capability of the proposed GPDD framework for UQ analysis under dependent random variables. Example 1 utilizes the four-step algorithm to assess the approximation accuracy of the measure-consistent orthogonal polynomials. Example 2 examines several analytical functions to illustrate the framework's effectiveness in statistical moment evaluation and reliability analysis. Example 3 focuses on the reliability assessment of a truss structure comprising 13 random variables.

For Examples 1 through 3, an isotropic Gauss quadrature scheme was used to construct the monomial moment matrix. In Example 1, the quadrature orders were chosen as 4, 14, and 40 for Cases 1, 2, and 3, respectively, based on convergence studies, whereas in the remaining two examples the corresponding orders were 16 (Case 1) and 33 (Case 2) for Example 2, and 65 for Example 3. In each example, the whitening matrix was obtained by applying the Cholesky factorization to the resulting moment matrix. The relative error is defined as the absolute value of the ratio between the difference of the approximate and benchmark solutions and the benchmark solution.

6.1. Example 1: Multivariate orthogonal polynomials

The first example focuses on generating measure-consistent orthogonal polynomials in subsets of three variables x_1, x_2 and x_3. Three distinct PDFs under Gaussian, Gegenbauer, and Dirichlet measures are considered to characterize the corresponding random variables X_1, X_2 and X_3, respectively, as follows.

1. Case 1: Gaussian PDF on $\mathbb{R}^3$:

$$f_{X_1,X_2,X_3}(\mathbf{x}) = (2\pi)^{-\frac{3}{2}} (\det \boldsymbol{\Sigma}_{\mathbf{X}})^{-\frac{1}{2}} \exp\left[-\tfrac{1}{2}\,\mathbf{x}^{\mathrm{T}}\boldsymbol{\Sigma}_{\mathbf{X}}^{-1}\mathbf{x}\right], \quad \mathbf{x} = (x_1, x_2, x_3)^{\mathrm{T}} \in \mathbb{R}^3, \tag{43}$$

where

$$\boldsymbol{\Sigma}_{\mathbf{X}} = \begin{bmatrix} \sigma_1^2 & \rho_{12}\sigma_1\sigma_2 & \rho_{13}\sigma_1\sigma_3 \\ \rho_{12}\sigma_1\sigma_2 & \sigma_2^2 & \rho_{23}\sigma_2\sigma_3 \\ \rho_{13}\sigma_1\sigma_3 & \rho_{23}\sigma_2\sigma_3 & \sigma_3^2 \end{bmatrix}, \quad \sigma_1 = \sigma_2 = \sigma_3 = \tfrac{1}{4}, \quad \rho_{12} = \rho_{13} = \rho_{23} = \tfrac{1}{5}.$$

2. Case 2: Gegenbauer PDF on $\mathbb{B}^3$:

$$f_{X_1,X_2,X_3}(\mathbf{x}) = \begin{cases} \dfrac{\Gamma(\mu+2)}{\pi^{\frac{3}{2}}\Gamma\left(\mu+\frac{1}{2}\right)}\left(1-\|\mathbf{x}\|^2\right)^{\mu-\frac{1}{2}}, & \mathbf{x} = (x_1, x_2, x_3)^{\mathrm{T}} \in \mathbb{B}^3, \\ 0, & \text{otherwise}, \end{cases} \tag{44}$$

where $\|\mathbf{x}\|^2 = \sum_{i=1}^{3} x_i^2$ and $\mu = 5$.

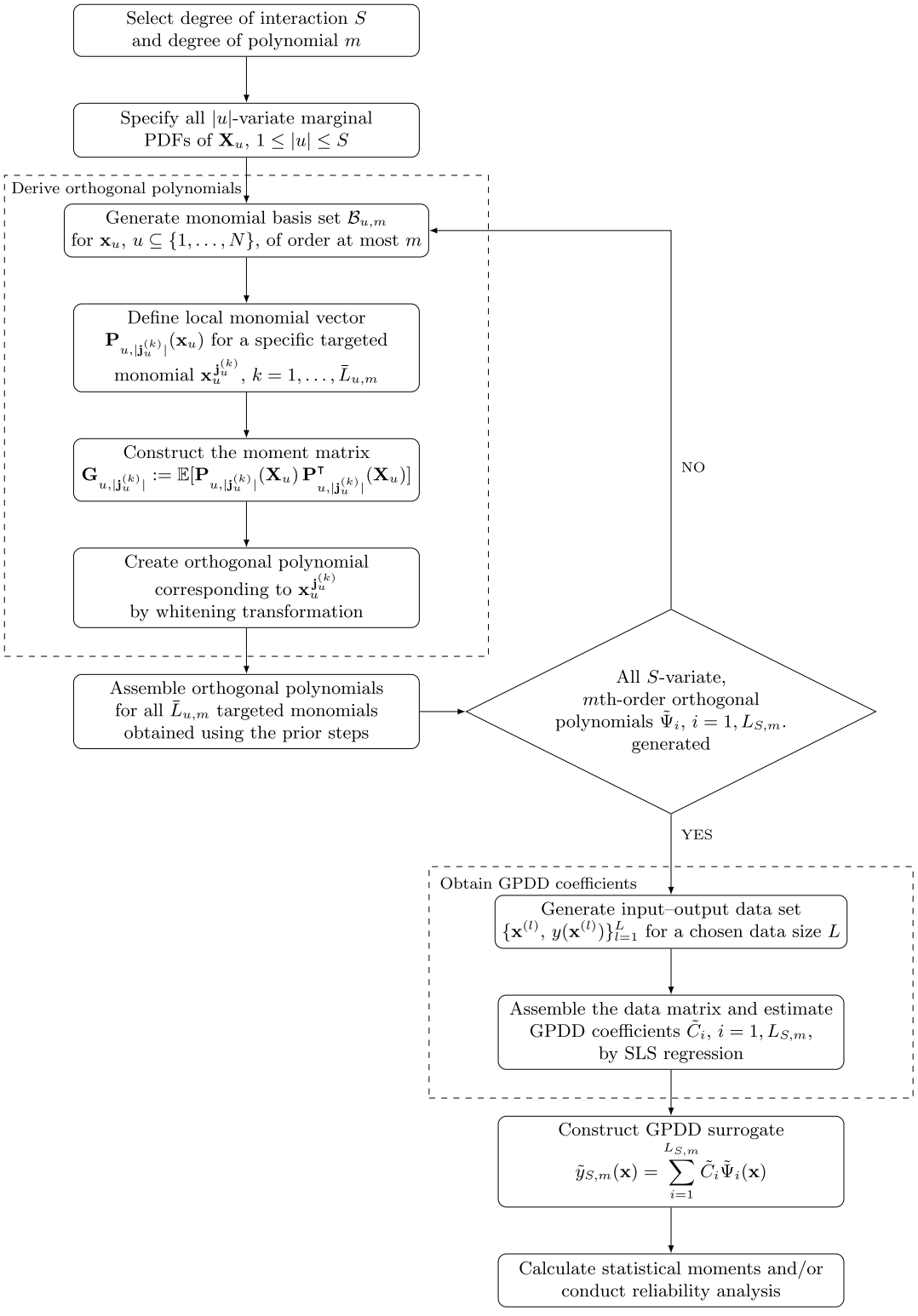

Fig. 1. A computational flow for generating a practical S-variate, mth-order GPDD approximation.

3. Case 3: Dirichlet PDF on $\mathbb{T}^3$:

$$f_{X_1,X_2,X_3}(\mathbf{x}) = \begin{cases} \dfrac{\Gamma\left(\sum_{i=1}^4 \kappa_i + 2\right)}{\prod_{i=1}^4 \Gamma(\kappa_i + \frac{1}{2})} \left(\prod_{i=1}^3 x_i^{\kappa_i - \frac{1}{2}} \right) (1 - |\mathbf{x}|)^{\kappa_4 - \frac{1}{2}}, & \mathbf{x} = (x_1, x_2, x_3)^{\mathrm{T}} \in \mathbb{T}^3, \\ 0, & \text{otherwise}, \end{cases} \tag{45}$$

where $|\mathbf{x}| = \sum_{i=1}^{3} x_i$ and $\kappa_1 = \kappa_2 = \kappa_3 = \kappa_4 = 1$.

Figs. 2, 3, and 4 display the joint and marginal PDFs described by (43), (44), and (45), respectively.

The Gaussian, Gegenbauer, and Dirichlet distributions were selected to evaluate the proposed algorithm across fundamentally different probability spaces – unbounded, bounded-symmetric, and bounded-simplex domains, respectively – thereby demonstrating its broad applicability. All three distributions admit a Rodrigues-type formula [15], which allows the exact analytical construction of measure-consistent orthogonal polynomials and provides a theoretical benchmark for verification.

In this work, the proposed four-step algorithm was applied to numerically construct measure-consistent orthogonal polynomials defined on subsets of random variables. The construction was performed dimensionwise; that is, univariate ($|u| = 1$), bivariate ($|u| = 2$), and trivariate ($|u| = 3$) orthogonal polynomials were generated sequentially using only the corresponding marginal probability distributions of the random input. For each probability measure, the monomial moment matrix was computed numerically using the isotropic Gauss quadrature scheme described in Section 5.1. In this approach, the transformed variables follow independent standard Gaussian distributions for unbounded rectangular domains (Case 1) and independent uniform distributions on $[0, 1]$ for bounded non-rectangular domains (Cases 2 and 3).

The orthogonal polynomials generated by the proposed algorithm for all three probability measures, up to total degree $m = 3$, are presented in Table B.1 of Appendix B. These numerically constructed polynomials exhibit excellent agreement with their analytical counterparts derived from the Rodrigues formula, as shown in Table B.2 of Appendix B [15]. Specifically, Tables B.1 and B.2 report all orthogonal polynomials in $\mathbf{x}_u$ for subsets $\emptyset \neq u \subseteq \{1, 2, 3\}$ with $1 \leq |u| \leq 3$, across all three probability measures considered. The indices satisfy $i \in \{1, 2, 3\}$ and $i_1, i_2 \in \{1, 2, 3\}$ with $i_2 > i_1$. It is readily verified that each polynomial listed in Table B.1 or Table B.2 fulfills, either approximately or exactly, the first- and second-order moment properties specified in (14)–(17).

6.2. Example 2: Two mathematical functions

The objective of the second example is to assess the effectiveness of GPDD in representing elementary mathematical functions when the expansion coefficients are estimated using the SLS regression technique. Two representative cases were examined, each involving a polynomial output function $y(X_1, X_2)$ of two statistically dependent input random variables X_1 and X_2, characterized by exponential and lognormal probability distributions, respectively. This example demonstrates that the GPDD approximations accurately preserve the statistical and probabilistic characteristics of the output functions under different non-product-type probability measures.

1. Case 1: A linear polynomial and exponential distribution

$$y(X_1, X_2) = 18 - 3X_1 - 2X_2,$$

$$f_{X_1X_2}(x_1, x_2) = \begin{cases} \exp[-(x_1 + x_2 + x_1x_2)][(1 + x_1)(1 + x_2) - 1], & 0 \leq x_1, x_2 < \infty, \\ 0, & \text{otherwise}. \end{cases}$$

2. Case 2: A quartic polynomial and lognormal-normal distribution

$$y(X_1, X_2) = 2500 - \frac{1}{2}(4X_1 - 5X_2^2)^2,$$

$$f_{X_1X_2}(x_1, x_2) = \begin{cases} \dfrac{50}{3\sqrt{19}\pi x_1} \exp\left[-\dfrac{50}{19} \left\{ \left(\dfrac{10 \ln x_1 - 20}{3} \right)^2 + \right. \right. \\ \left. \left. (x_2 - 1)^2 + \dfrac{9}{5} \left(\dfrac{10 \ln x_1 - 20}{3} \right)(x_2 - 1) \right\} \right], & 0 \leq x_1 < \infty; -\infty < x_2 < \infty \\ 0, & \text{otherwise}. \end{cases}$$

For the GPDD analysis, the degree of interaction (S) and polynomial order (m) were selected according to the levels of cross terms and nonlinearity present in the output function. For example, Case 1, which involves a linear function with no cross terms, requires only a first-order expansion ($m = 1$) and thus employs solely univariate basis functions. In contrast, Case 2 exhibits nonlinear interactions between the input variables and therefore necessitates a fourth-order expansion ($m = 4$), incorporating both univariate and bivariate basis functions to adequately capture higher-order effects. Consequently, the numbers of GPDD basis functions ($L_{S,m}$) for Cases 1 and 2 are 3 and 15, respectively.

The ratio ($L/L_{S,m}$) used in the SLS regression ranges from 1 to 2, determined empirically through trial and error. Benchmark values for the mean and standard deviation of $y(X_1, X_2)$ serve as reference targets for verifying the GPDD approximations. In Case 1, the exact

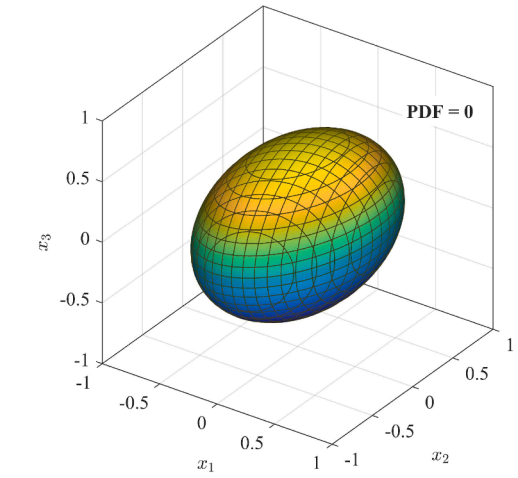

(a)

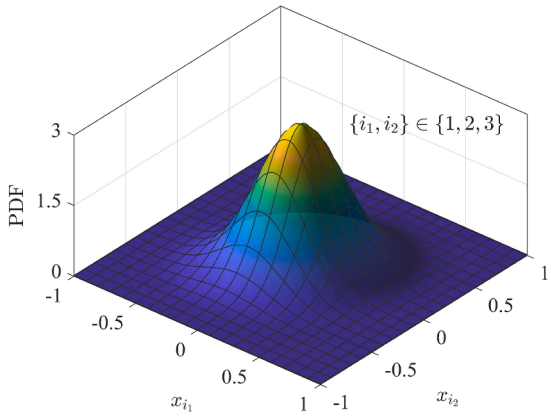

(b)

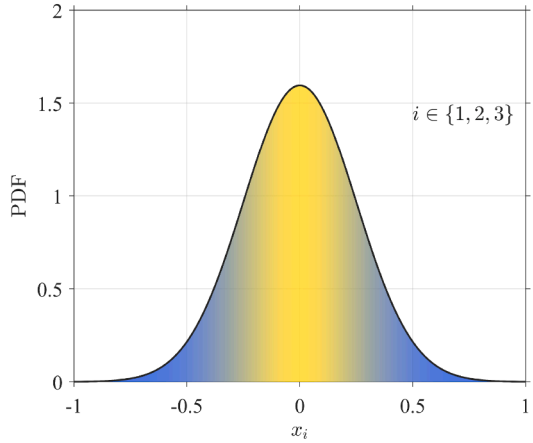

(c)

Fig. 2. Gaussian PDF on $\mathbb{R}^3$ with distribution parameters: $\sigma_1 = \sigma_2 = \sigma_3 = \frac{1}{4}$, $\rho_{12} = \rho_{13} = \rho_{23} = \frac{1}{5}$; (a) contour plot of $f_{X_1X_2X_3}(x_1, x_2, x_3) = 0$; (b) bivariate marginal densities of (X_i, X_j); (c) univariate marginal densities of X_i.

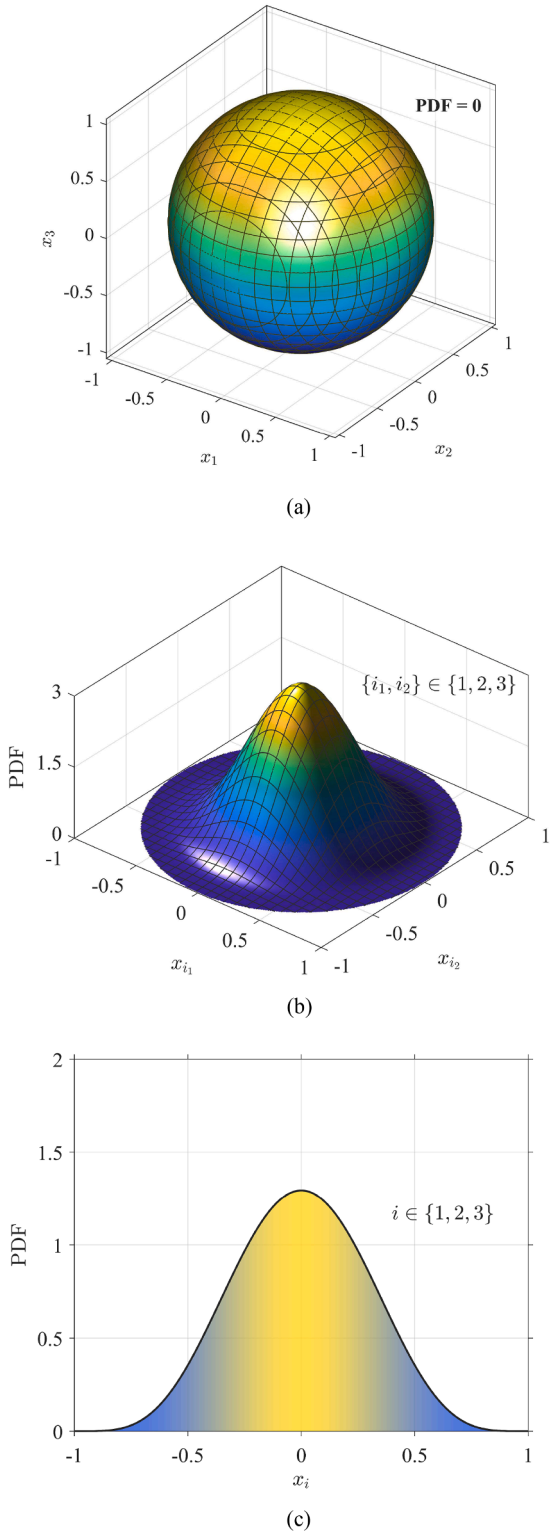

Fig. 3. Gegenbauer PDF on $\mathbb{B}^3$ with distribution parameter: $\mu = 5$; (a) contour plot of $f_{X_1X_2X_3}(x_1, x_2, x_3) = 0$; (b) bivariate marginal densities of (X_i, X_j); (c) univariate marginal densities of X_i.

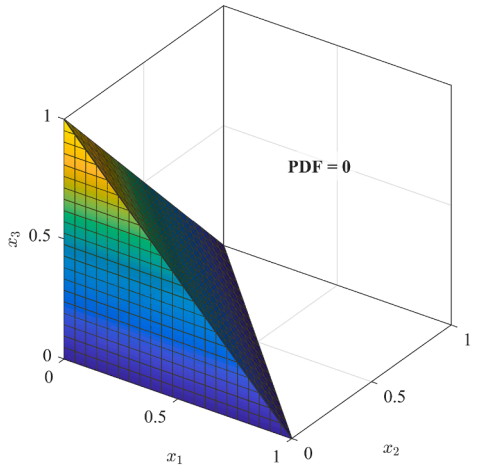

(a)

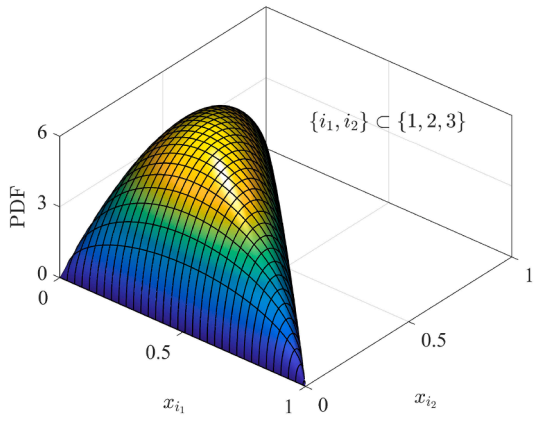

(b)

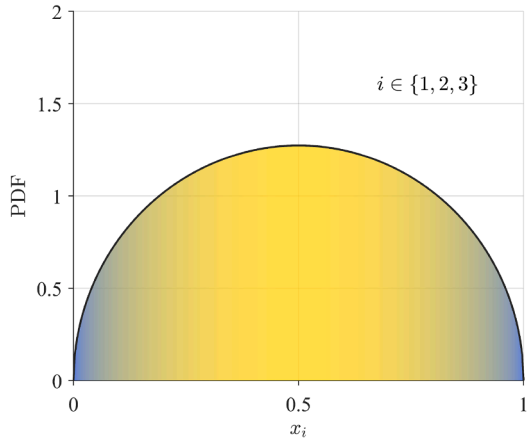

(c)

Fig. 4. Dirichlet PDF on $\mathbb{T}^3$ with distribution parameters: $\kappa_1 = \kappa_2 = \kappa_3 = \kappa_4 = 1$; (a) contour plot of $f_{X_1X_2X_3}(x_1, x_2, x_3) = 0$; (b) bivariate marginal densities of (X_i, X_j); (c) univariate marginal densities of X_i.

Table 1
Relative errors in the second-moment properties of two functions by GPDD, GPCE, and PCE (Example 2).

	Relative error[a]		
	Mean	Standard deviation	No. of function evaluations[b]
(1) Case 1: A linear polynomial and exponential distribution			
Univarite, 1st-order GPDD	1.0×10^{-15}	1.4×10^{-5}	3
1st-order GPCE	1.4×10^{-15}	1.5×10^{-5}	3
5th-order PCE	1.3×10^{-6}	2.0×10^{-4}	144
6th-order PCE	4.8×10^{-7}	5.6×10^{-5}	196
7th-order PCE	1.5×10^{-7}	3.7×10^{-5}	256
(2) Case 2: A quartic polynomial and lognormal-normal distribution			
Bivariate, 4th-order GPDD	3.9×10^{-8}	1.7×10^{-7}	15
4th-order GPCE	4.5×10^{-8}	1.8×10^{-7}	15
4th-order PCE	4.4×10^{-8}	1.9×10^{-6}	25
5th-order PCE	9.7×10^{-9}	2.0×10^{-6}	36
6th-order PCE	9.0×10^{-9}	3.5×10^{-7}	49

[a] The benchmark solutions for Case 1 and Case 2 are exact and crude MCS (10^6 samples), respectively.
[b] The total number of times the original output function is calculated.

mean and standard deviation are 13.00000 and 2.85594, respectively, while in Case 2 they are 2089.03370 and 378.68671, obtained using crude MCS with a million samples. These reference statistics provide a quantitative basis for determining how accurately the GPDD approximations reproduce the true solutions.

6.2.1. Statistical moment analysis

The relative errors in the mean and standard deviation of $y(X_1, X_2)$ committed by the GPDD approximations for both cases, together with the corresponding numbers of function evaluations, are summarized in Table 1. For comparison, Table 1 also includes reference solutions as well as approximate results produced by GPCE [31] and classical tensor-product PCE [31]. According to the table, GPDD achieves the lowest errors for estimating both the mean and standard deviations of $y(X_1, X_2)$ for the two cases considered. Although the output functions are polynomial, the GPDD errors do not vanish completely because both the expansion coefficients and the orthogonal polynomials are obtained numerically. Nonetheless, these errors remain negligibly small, particularly in view of the relatively modest number of function evaluations used to estimate the GPDD coefficients. It is also noteworthy that GPCE yields results of comparable quality for this low-dimensional problem.

In contrast, classical tensor-product PCE, when combined with a Rosenblatt transformation to map dependent variables into independent ones, produces highly nonlinear, non-polynomial output functions. As a result, achieving the same level of accuracy in estimating the standard deviation by GPDD or GPCE often requires a sixth- or seventh-order PCE, depending on the specific function. Consequently, the number of function evaluations required for classical PCE increases by an order of magnitude. By directly handling dependent variables, GPDD and GPCE not only avoid the need for measure transformations but also provide accurate estimates of the second-moment properties of the output functions while maintaining a low computational cost.

6.2.2. Reliability analysis

Table 2 presents the estimated failure probabilities $\mathbb{P}[y(\mathbf{X}) < 0]$ and requisite numbers of function evaluations for both output functions obtained using the proposed GPDD, alongside the corresponding reference values derived from crude MCS or exact analytical solutions. Consistent with the statistical moment analysis, the GPDD-based estimates show excellent agreement with the reference solutions, highlighting the framework's accuracy in probabilistic failure assessment for globally smooth output functions.

For comparison with existing approaches, the classical first-order reliability method (FORM) [34] was also applied to solve this problem. However, the FORM results prove to be less straightforward due to the occurrence of multiple most probable points (MPPs) and the non-uniqueness of the Rosenblatt transformation. As a result, several distinct failure probability estimates by FORM are needed, as summarized in Table 2. While some of the FORM-based estimates are accurate, others deviate substantially, and without benchmark data from MCS or exact solutions, it is difficult to identify which estimate is credible. In contrast, GPDD yields unique, stable, and consistent estimates across all cases without suffering from the ambiguity inherent in FORM. Notably, although FORM is widely recognized for its computational efficiency, GPDD attains comparable or superior accuracy at a lower computational cost, demonstrating its robustness and effectiveness in reliability analysis involving dependent random variables.

To assess the accuracy of the GPDD framework in calculating rare-event failure probabilities, the original output functions in Cases 1 and 2 have been modified as follows: (1) Modified Case 1: $y(\mathbf{X}) = 40 - 3X_1 - 2X_2$ and (2) Modified Case 2: $y(\mathbf{X}) = 10000 - \frac{1}{2}(4X_1 - 5X_2^2)^2$. The input probability distributions are the same as described earlier in Section 6.2. The estimated failure probabilities for these two modified output functions and the corresponding numbers of function evaluations obtained using the aforementioned three methods are summarized in Table 3. The results demonstrate that GPDD can accurately and efficiently estimate rare-event failure probabilities in problems involving dependent random variables, while avoiding the ambiguity and computational burden associated with conventional reliability methods.

Table 2
Failure probabilities associated with two performance functions calculated by GPDD and other methods (Example 2).

Method	Failure probability $\mathbb{P}[y(\mathbf{X}) < 0]$[a]	No. of function evaluations[b]
(1) Case 1: A linear polynomial and exponential distribution		
Uivariate, 1st-order GPDD[c]	2.91×10^{-3}	3
Crude MCS	3.02×10^{-3}	$1,000,000$
FORM		
Transformation 1[d]		
1st MPP	2.70×10^{-3}	35[e]
2nd MPP	2.32×10^{-4}	35[e]
Transformation 2[f]		
1st MPP	4.00×10^{-3}	45[e]
2nd MPP	1.40×10^{-4}	45[e]
Exact	2.95×10^{-3}	
(2) Case 2: A quartic polynomial and lognormal-normal distribution		
Bivariate, 4th-order GPDD[c]	1.08×10^{-3}	15
Crude MCS	1.10×10^{-3}	$1,000,000$
FORM		
Transformation 1[d]		
1st MPP	1.52×10^{-4}	42[e]
2nd MPP	1.00×10^{-3}	42[e]

a. $y(\mathbf{X}) = 18 - 3X_1 - 2X_2$ for Case 1; $y(\mathbf{X}) = 2500 - \frac{1}{2}(4X_1 - 5X_2^2)^2$ for Case 2.
b. The total number of times the original output function is calculated.
c. MCS of GPDD approximation (10^6 samples).
d. $T_1 \equiv (x_1, x_2) \rightarrow (u_1, u_2)$ on standard Gaussian space.
e. The number of function evaluations to find both MPPs.
f. $T_2 \equiv (x_2, x_1) \rightarrow (u_1, u_2)$ on standard Gaussian space.

Table 3
Rare-event failure probabilities associated with two modified performance functions calculated by GPDD and other methods (Example 2).

Method	Failure probability $\mathbb{P}[y(\mathbf{X}) < 0]$[a]	No. of function evaluations[b]
(1) Modified Case 1: A linear polynomial and exponential distribution		
Uivariate, 1st-order GPDD[c]	1.66×10^{-6}	3
Crude MCS	1.82×10^{-6}	$100,000,000$
FORM		
Transformation 1[d]		
1st MPP	1.57×10^{-6}	35[e]
2nd MPP	9.32×10^{-9}	35[e]
Exact	1.70×10^{-6}	
(2) Modified Case 2: A quartic polynomial and lognormal-normal distribution		
Bivariate, 4th-order GPDD[c]	3.56×10^{-6}	15
Crude MCS	3.58×10^{-6}	$100,000,000$
FORM		
Transformation 1[d]		
1st MPP	3.32×10^{-6}	42[e]
2nd MPP	9.31×10^{-13}	42[e]

a. $y(\mathbf{X}) = 40 - 3X_1 - 2X_2$ for Case 1; $y(\mathbf{X}) = 10000 - \frac{1}{2}(4X_1 - 5X_2^2)^2$ for Case 2.
b. The total number of times the original output function is calculated.
c. MCS of GPDD approximation (10^8 samples).
d. $T_1 \equiv (x_1, x_2) \rightarrow (u_1, u_2)$ on standard Gaussian space.
e. The number of function evaluations to find both MPPs.

6.3. Example 3: A 13-bar truss

In this final example, a linear-elastic, 13-bar truss structure was analyzed to evaluate the accuracy and computational efficiency of the proposed GPDD framework in structural reliability assessment. As illustrated in Fig. 5, the truss is simply supported at nodes 1 and 8 and is subjected to three vertically downward concentrated loads of 85,000 lb, 100,000 lb, and 85,000 lb applied at nodes 3,

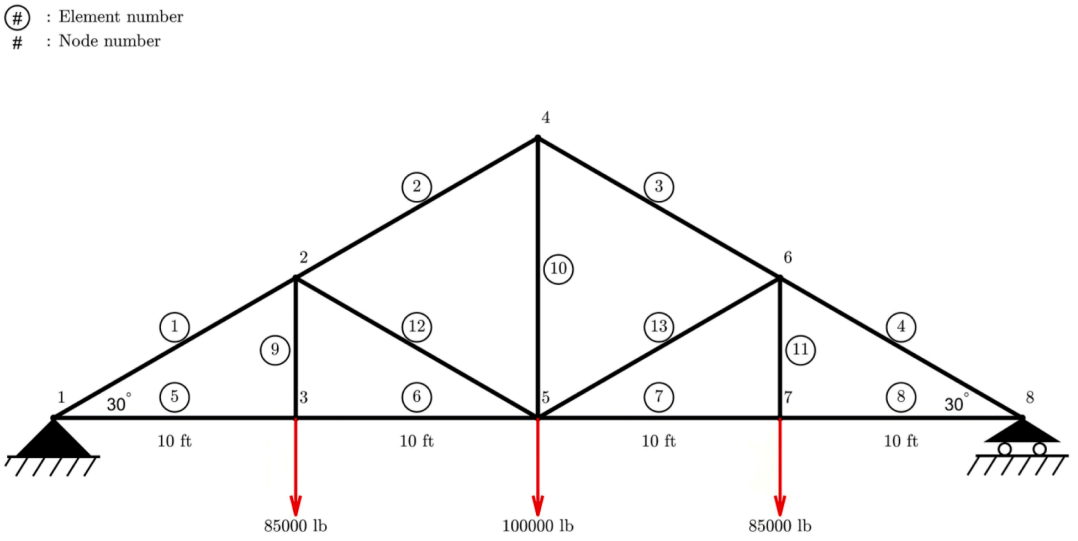

Fig. 5. A 13-bar truss structure (Example 3).

5, and 7, respectively. Each panel has a horizontal span of 10 ft, and all diagonal members are inclined at 30 degrees. The truss is made of structural steel with a Young's modulus $E = 30 \times 10^6$ psi and Poisson's ratio $\nu = 0.3$. The yield strength is 30,000 psi, with an allowable stress limit of 20,000 psi.

The cross-sectional areas of all 13 members were modeled as a correlated truncated lognormal random vector $\mathbf{X} = (X_1, \ldots, X_{13})^\intercal$, with each component having identical means $\mu_i = 22$ in^2, standard deviations $\sigma_i = 3.5$ in^2, and correlation coefficients $\rho_{ij} = 0.42$ for $i, j = 1, \ldots, 13$, $i \neq j$. A deterministic FEA identifies the maximum vertical deflection $v_5(\mathbf{X})$ at node 5 (mid-span), with an allowable limit of 0.6 in. The maximum axial stress $\sigma_4(\mathbf{X})$ occurs in bar 4, connecting nodes 6 and 8, with an allowable stress of 20,000 psi. Accordingly, two performance functions, defined as

$$y_1(\mathbf{X}) = 0.6 - v_5(\mathbf{X}), \qquad y_2(\mathbf{X}) = 20{,}000 - \sigma_4(\mathbf{X}),$$

represent the displacement- and stress-based limit-state functions, respectively. The corresponding failure probabilities are then defined as

$$P_{F,1} := \mathbb{P}[y_1(\mathbf{X}) < 0], \qquad P_{F,2} := \mathbb{P}[y_2(\mathbf{X}) < 0].$$

The objective of this example is to estimate these two failure probabilities using the GPDD approximation, as outlined in Section 5.3, in conjunction with the SLS regression for obtaining the expansion coefficients.

Table 4 presents the estimated failure probabilities of the truss structure, computed using four GPDD approximations and crude MCS with a sample size of 100,000. The GPDD involves: (1) univariate, second-order ($S = 1$, $m = 2$); (2) (1) univariate, third-order ($S = 1$, $m = 3$); (3) bivariate, second-order ($S = 2$, $m = 2$); and (4) bivariate, third-order ($S = 2$, $m = 3$) approximations. For each GPDD approximation, the data size L was selected as approximately 2.2 times the total number of basis functions $L_{S,m}$ to ensure numerical stability and accuracy of the SLS regression in estimating the corresponding GPDD coefficients. The factor 2.2 was established empirically by trial and error.

As shown in Table 4, all four GPDD variants accurately predict the order of magnitude of the failure probabilities obtained from crude MCS, regardless of the performance function. In particular, the bivariate, third-order GPDD approximations yield highly accurate estimates of failure probability for both displacement- and stress-based limit-state functions, requiring only a few hundred FEA.

7. Application

This section illustrates the application of GPDD to a high-dimensional, real-world engineering problem from the automotive industry. Specifically, it addresses the stochastic stress analysis of the lower control arm (LCA) in the front suspension system of a vehicle.

7.1. Geometry and CAD model

As illustrated in Fig. 6(a), the LCA is a critical component of the suspension system, connecting the vehicle chassis to the wheel assembly (knuckle) via two bushing mounts and a ball-joint housing. It plays a key role in maintaining stability, ensuring proper wheel alignment, and enabling the suspension to absorb shocks, thereby contributing to a safe and comfortable ride. Given that

Table 4
Two failure probabilities of the truss structure calculated by GPDD and crude MCS (Example 3).

Method	Failure probability $\mathbb{P}[y_1(\mathbf{X}) < 0]$[a]	Failure probability $\mathbb{P}[y_2(\mathbf{X}) < 0]$[b]	No. of coefficients	Number of FEA
Univariate GPDD				
2nd-order, $m = 2$	2.70×10^{-4}	1.29×10^{-3}	27	60
3rd-order, $m = 3$	6.26×10^{-4}	3.71×10^{-3}	40	88
Bivariate GPDD				
2nd-order, $m = 2$	3.32×10^{-4}	1.36×10^{-3}	105	231
3rd-order, $m = 3$	6.31×10^{-4}	2.67×10^{-3}	274	603
Crude MCS	6.60×10^{-4}	2.74×10^{-3}		100,000

a. $y_1(\mathbf{X}) = 0.6 - v_5(\mathbf{X})$.
b. $y_2(\mathbf{X}) = 20,000 - \sigma_4(\mathbf{X})$.

the LCA is subjected to severe operating conditions, including repeated road impacts, vibrations, and cyclic deformations, engineers routinely conduct stress analyses to evaluate its structural integrity and fatigue performance.

Fig. 6(b) and (c) present the computer-aided design (CAD) model of the LCA, incorporating 31 random geometric variables, denoted by X_1 through X_{31}, which represent wall thicknesses, rib dimensions, hole sizes, and fillet radii throughout the structure.

7.2. Finite-element model and random input

Due to the complex geometry of the LCA, numerical analyses, such as FEA, are essential for evaluating its deformation and stress responses. Fig. 7(a) depicts the loading and boundary conditions applied for a quasi-static, linear-elastic FEA of the LCA using the ABAQUS commercial software [35]. The LCA material is assumed to be isotropic with random variations in Young's modulus X_{32} and Poisson's ration X_{33}. A random vertical load X_{34} was applied on the LCA body to simulate a downward force transmitted from the vehicle in response to a severe road input acting on the suspension assembly. The two bushing sleeves were fixed in the global coordinate system to replicate the chassis-mounted constraints. A fully automated CAD-FEA interface was developed such that, for any selected set of geometric parameters, the CAD model is regenerated, meshed, and analyzed in ABAQUS. For the mean values of the input variables, the resulting FEA model consists of approximately 60,000 tetrahedral elements, as shown in Fig. 7(b).

The input random vector for this problem is defined as $\mathbf{X} = (X_1, \dots, X_{34})^\intercal$, representing a total of 34 uncertain parameters. The means and coefficients of variation of these variables, based on practical considerations, are summarized in Table 5. The pairwise correlation coefficients among the geometric variables ($X_1 - X_{31}$) and between the material properties (X_{32}, X_{33}) are both equal to $\rho = 0.3$. However, the groups of geometric variables, material properties, and load are statistically independent from one another. It is further assumed that $\mathbf{X}$ follows a right-truncated lognormal distribution, where each variable X_i is truncated at its mean plus six times its standard deviation. Given the large truncation limit, the truncated and untruncated lognormal distributions are effectively indistinguishable for practical purposes. Most existing methods, including GPCE, are susceptible to the curse of dimensionality [36] and thus encounter significant challenges when addressing this high-dimensional UQ problem.

For the GPDD-based UQ analysis of the LCA, the monomial moment matrix was constructed using an isotropic Gauss quadrature scheme. A quadrature order of 65 was selected for this case based on convergence studies, and the corresponding whitening matrix was obtained through the Cholesky factorization of the resulting moment matrix.

7.3. Deformation and stress analysis

For the output quantities of interest, two response measures frequently used in stress and fatigue durability analysis were studied: (1) the von Mises stress and (2) the largest principal strain in the LCA. When all input variables are fixed at their mean values, the contour plots of these responses indicate that the maximum Von Mises stress or the maximum largest principal strain occurs near the corner of the rear bushing joint, where the control arm is connected to the chassis, as displayed in Fig. 8(a) or (b). In the presence of input uncertainty, however, these response measures become random variables or fields. In this work, GPDD was employed to characterize the statistical behavior of these responses under combined effects of geometric, material, and loading uncertainties.

Table 6 summarizes the approximate means and standard deviations of the maximum von Mises stress and maximum largest principal strain, obtained using three GPDD approximations: (1) univariate, second-order ($S = 1$, $m = 2$); (2) univariate, third-order ($S = 1$, $m = 3$); and (3) bivariate, second-order ($S = 2$, $m = 2$). As shown in the table, all three GPDD variants provide good to excellent estimates of the second-moment statistics of the stress or strain when compared with results from crude MCS using 7000 samples. While the bivariate GPDD yields the most accurate solution, it is also the most computationally expensive, requiring 3150 FEA. In contrast, the univariate, third-order GPDD produces results nearly identical to those of the bivariate approximation while incurring only 515 FEA.

Finally, Fig. 9(a) and (b) present the approximate PDFs of the maximum von Mises stress and maximum largest principal strain obtained using the three GPDD approximations described earlier, while Fig. 9(c) and (d) show the corresponding approximate CDFs. The GPDD-derived PDFs or CDFs were generated by resampling the GPDD approximations 10,000 times. The computational cost of this resampling is negligible, as it involves only evaluations of the elementary polynomial functions defining the GPDD approximations, and should not be confused with crude MCS of the actual responses. Due to the high computational expense of performing FEA, the

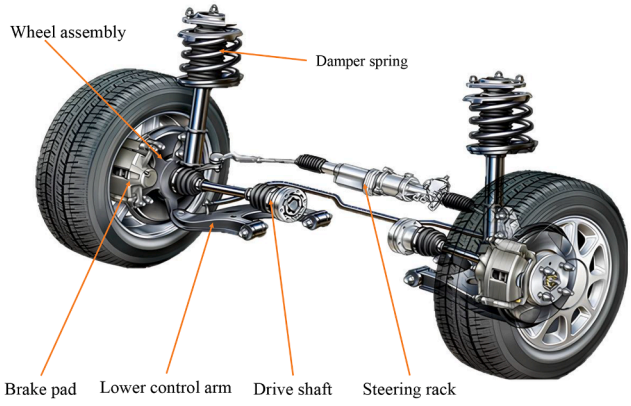

(a)

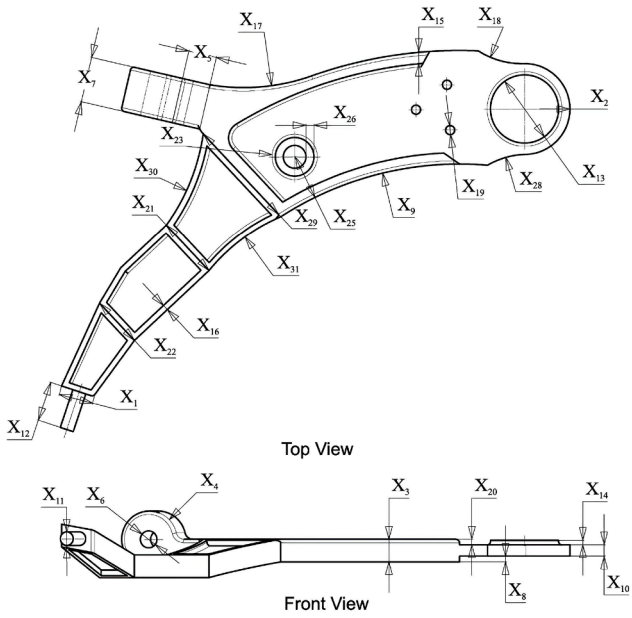

(b)

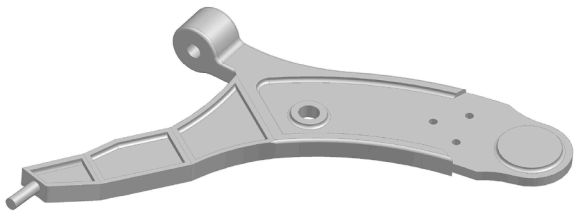

(c)

Fig. 6. A lower control arm of vehicle's suspension system; (a) suspension system assembly; (b) top and front views of CAD model; (c) isometric view of CAD model.

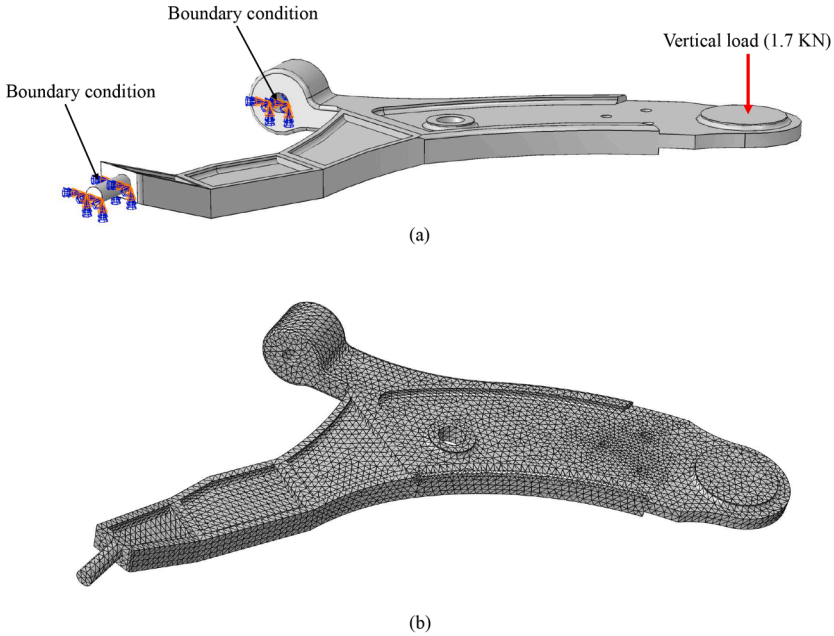

Fig. 7. Loading and boundary conditions and FEA discretization of the LCA; (a) loading and boundary conditions; (b) tetrahedral mesh from ABAQUS (60,000 elements).

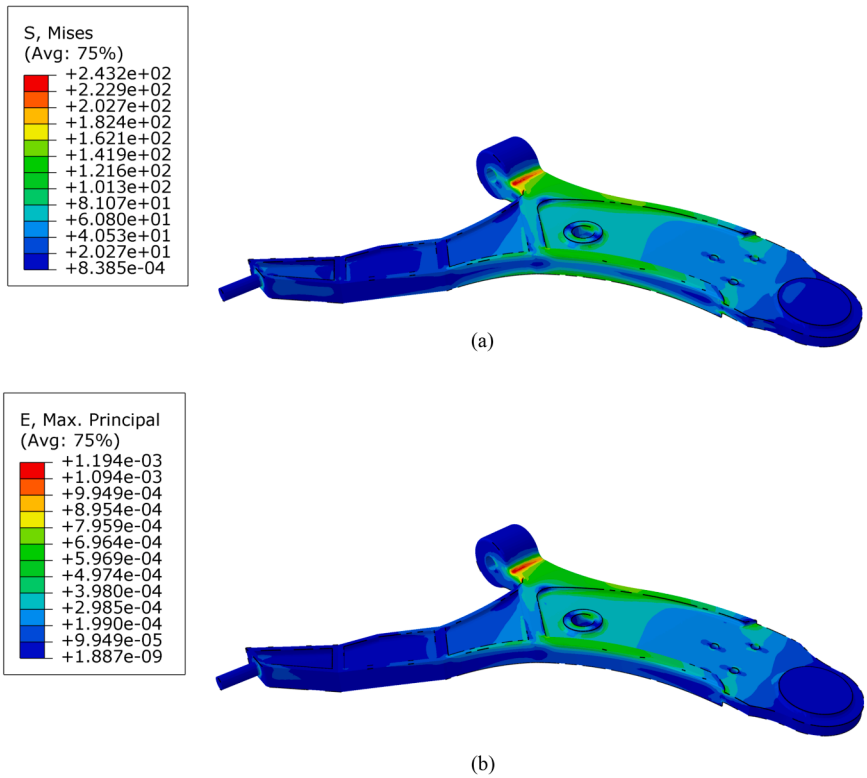

Fig. 8. Results of deterministic FEA at mean input for the LCA; (a) contours of von Mises stress; (b) contours of largest principal strain.

Table 5
Statistical properties of 34 input random variables for the LCA.

Variable	Mean (μ)	Coefficient of Variation (%)
(a) Geometric variables		
X_1	30 (mm)	7
X_2	40 (mm)	7
X_3	20 (mm)	7
X_4	25 (mm)	7
X_5	15 (mm)	7
X_6	25 (mm)	7
X_7	40 (mm)	7
X_8	5 (mm)	7
X_9	290 (mm)	7
X_{10}	10 (mm)	7
X_{11}	12 (mm)	7
X_{12}	35 (mm)	7
X_{13}	60 (mm)	7
X_{14}	4 (mm)	7
X_{15}	10 (mm)	7
X_{16}	5 (mm)	7
X_{17}	180 (mm)	7
X_{18}	70 (mm)	7
X_{19}	8 (mm)	7
X_{20}	5 (mm)	7
X_{21}	55 (mm)	7
X_{22}	45 (mm)	7
X_{23}	20 (mm)	7
X_{24}	4 (mm)	7
X_{25}	35 (mm)	7
X_{26}	7 (mm)	7
X_{27}	70 (deg)	7
X_{28}	80 (deg)	7
X_{29}	180 (mm)	7
X_{30}	185 (mm)	7
X_{31}	170 (mm)	7
(b) Material variables		
X_{32}	210 (GPa)	7
X_{33}	0.3	7
(c) Force variable		
X_{34}	1.7 (kN)	15

(a) Geometric variables X_1–X_{31} follow pairwise correlation $\rho = 0.3$.
(b) Material variables X_{32} and X_{33} follow correlation $\rho = 0.3$.
(c) Vertical load X_{34} is independent of all others.

Table 6
Second-moment properties of two response measures of the LCA by GPDD and crude MCS.

	Max. von Mises stress (MPa)		Max. largest prin. strain (%)		
Method	Mean	Standard deviation	Mean	Standard deviation	Number of FEA
Univariate GPDD					
2nd-order, $m = 2$	234.54	51.91	0.00111	2.68×10^{-4}	345
3rd-order, $m = 3$	234.89	54.13	0.00109	2.69×10^{-4}	515
Bivariate GPDD					
2nd-order, $m = 2$	235.12	53.91	0.00115	2.78×10^{-4}	3,150
Crude MCS	235.17	53.85	0.00116	2.74×10^{-4}	7,000

same 7000 realizations of stress and strain were used to generate the referential densities and distributions, which are also plotted in Figs. 9(a) through 9(d). Given the limited sample size, the MCS-generated distributions are not expected to accurately capture tail probabilistic behavior. Nevertheless, the overall trends of the PDFs and CDFs obtained obtained from the bivariate, second-order GPDD closely match the MCS results. In contrast, while the univariate, second- or third-order GPDD provides accurate CDF estimates for probabilities down to approximately 0.01, it deviates from the bivariate GPDD and MCS results at lower probabilities. This comparison underscores the importance of incorporating bivariate interactions in GPDD when evaluating the tail probabilistic characteristics of output variables, albeit at the cost of increased computational effort. Consequently, the development of an adaptive

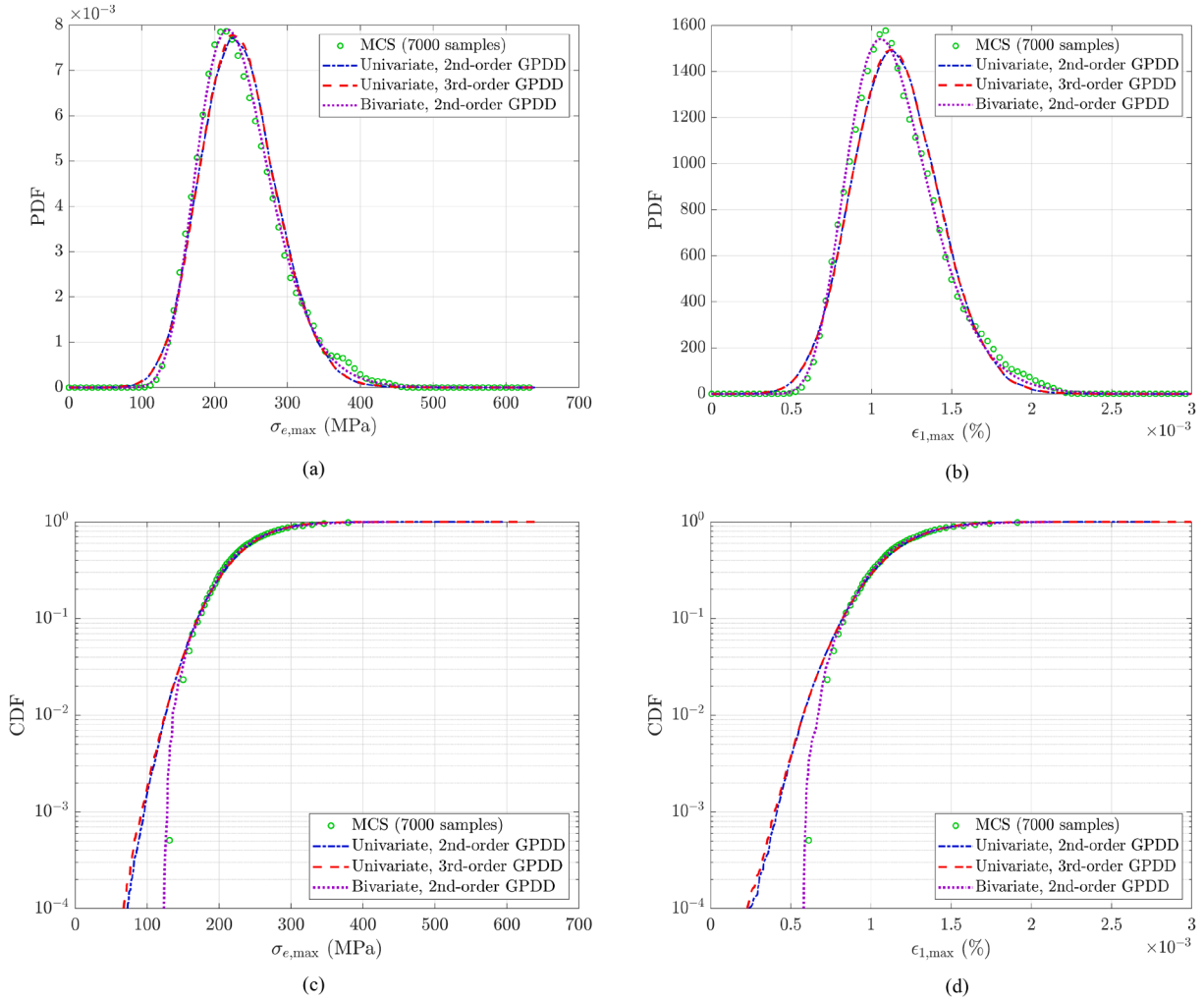

Fig. 9. Probability distribution functions of two responses for the LCA; (a) PDF of maximum von Mises stress $\sigma_{e,\max}$; (b) PDF of maximum largest principal strain $\epsilon_{1,\max}$; (c) CDF of maximum von Mises stress $\sigma_{e,\max}$; (d) CDF of maximum largest principal strain $\epsilon_{1,\max}$.

GPDD variant – one capable of automatically identifying and including only the most influential bivariate interactions – warrants further investigation to achieve additional reductions in computational cost.

8. Outlook

While this paper presents a practical implementation of GPDD for dependent variables, its scope is limited to forward UQ analysis. Several challenges remain in addressing inverse UQ problems, such as those encountered in design optimization under uncertainty: (1) determining the design sensitivities of statistical moments or reliability without incurring significant additional computational cost; (2) minimizing or avoiding repetitive calculations of moments, reliability, and their design sensitivities during iterative design processes; and (3) substantially reducing the number of function evaluations or FEA simulations required in conjunction with standard gradient-based optimization algorithms. Addressing these challenges will be the focus of future work by the authors.

9. Conclusion

A new practical GPDD framework was devised to enable efficient UQ analysis when the input random variables are statistically dependent and follow a general, non-product-type probability distribution. The key intellectual contribution of this framework is an innovative four-step algorithm for constructing multivariate orthogonal polynomials from scratch, in subsets of input variables, that are consistent with the specified input probability distribution. Unlike the Rodrigues-type formula, which is limited to certain probability measures, the proposed algorithm can generate orthogonal polynomials for a broader class of input distributions, heretofore unavailable to the UQ community.

In contrast to GPCE, which requires the full joint distribution of the random inputs to generate orthogonal polynomials, GPDD relies only on low-variate marginal distributions. Consequently, when the joint distribution is unknown but the marginal distributions are available, a GPDD approximation can still be constructed in a dimensionwise manner, facilitating efficient UQ analysis. For high-dimensional stochastic problems characterized by strongly nonlinear output functions but weak interactions among input variables, GPDD is expected to be significantly more computationally efficient than GPCE, owing to its hierarchical, dimensionwise structure – a feature not present in GPCE.

Numerical results of the proposed algorithm for generating orthogonal polynomials consistent with Gaussian, Gegenbauer, and Dirichlet probability distributions demonstrate high accuracy when compared with exact solutions from Rodrigues' formula. More important, UQ analysis of two mathematical functions and a truss structure indicate that GPDD, combined with standard least-squares regression for calculating the expansion coefficients, provides excellent estimates of the second-moment properties and reliability using only a few hundred function evaluations or finite element analyses. Furthermore, application to an industrial-scale problem demonstrates GPDD's practical utility, integrating seamlessly with legacy simulation code to perform high-dimensional UQ analysis of a vehicle suspension control arm entailing 34 input variables.

CRediT authorship contribution statement

Md Rashel Talukdar: Writing – review & editing, Writing – original draft, Visualization, Validation, Methodology, Investigation, Formal analysis, Data curation; **Sharif Rahman:** Writing – review & editing, Writing – original draft, Supervision, Project administration, Methodology, Investigation, Funding acquisition, Formal analysis, Conceptualization.

Data availability

Data will be made available on request.

Declaration of competing interest

The authors declare that they have no known competing financial interests or personal relationships that could have appeared to influence the work reported in this paper.

Acknowledgement

Grant sponsor: U.S. National Science Foundation (Grant No. CMMI-2317172).

Appendix A. Generation of orthogonal polynomials by four-step algorithm

Let $(X_1, X_2)^{\mathsf{T}}$ be a random vector comprising *zero*-mean Gaussian random variables, which have identical standard deviations $\sigma_1 = \sigma_2 = \frac{1}{4}$ and correlation coefficient $\rho = \frac{1}{5}$. For $u = \{1, 2\}$ and $m = 3$, the index sets with graded reverse lexicographic order and respective cardinalities, as defined in Step 1, are

$$\mathcal{I}_{\{1,2\},3} = \{(0,0),(1,0),(0,1),(2,0),(1,1),(0,2),(3,0),(2,1),(1,2),(0,3)\};\ L_{\{1,2\},3} = |\mathcal{I}_{\{1,2\},3} = 10,$$
$$\bar{\mathcal{I}}_{\{1,2\},3} = \{(1,1),(2,1),(1,2)\};\ \bar{L}_{\{1,2\},3} = |\bar{\mathcal{I}}_{\{1,2\},3}| = 3,$$

producing the associated monomial set

$$\mathcal{B}_{\{1,2\},3} = \{1,\ x_1,\ x_2,\ x_1^2,\ x_1x_2,\ x_2^2,\ x_1^3,\ x_1^2x_2,\ x_1x_2^2,\ x_2^3\}.$$

There are three multi-index values in $\bar{\mathcal{I}}_{\{1,2\},3}$, meaning that a total of three bivariate orthogonal polynomials have to be generated. For such multi-index values $\mathbf{j}_{\{1,2\}}^{(k)}$, $k = 1, 2, 3$, the reduced index sets $\mathcal{I}_{\{1,2\},|\mathbf{j}_{\{1,2\}}^{(k)}|}$, their cardinalities, and local monomial vectors, as defined in Step 2, are as follows:

1. $k = 1$: $\mathbf{j}_{\{1,2\}}^{(1)} = (1,1)$, $|\mathbf{j}_{\{1,2\}}^{(1)}| = 2$

$$\mathcal{I}_{\{1,2\},|\mathbf{j}_{\{1,2\}}^{(1)}|} = \{(0,0),(1,0),(0,1),(2,0),(0,2),(1,1)\},\ \left|\mathcal{I}_{\{1,2\},|\mathbf{j}_{\{1,2\}}^{(1)}|}\right| = 6,$$
$$\mathbf{P}_{\{1,2\}\mathbf{j}_{\{1,2\}}^{(1)}}(x_1,x_2) = \left(1,\ x_1,\ x_2,\ x_1^2,\ x_2^2,\ x_1x_2\right)^{\mathsf{T}},$$

   with the targeted monomial x_1x_2 as the last element.
2. $k = 2$: $\mathbf{j}_{\{1,2\}}^{(2)} = (2,1)$, $|\mathbf{j}_{\{1,2\}}^{(2)}| = 3$

$$\mathcal{I}_{\{1,2\},|\mathbf{j}_{\{1,2\}}^{(2)}|} = \{(0,0),(1,0),(0,1),(2,0),(1,1),(0,2),(3,0),(1,2),(0,3),(2,1)\},\ \left|\mathcal{I}_{\{1,2\},|\mathbf{j}_{\{2,1\}}^{(2)}|}\right| = 10,$$
$$\mathbf{P}_{\{1,2\}\mathbf{j}_{\{2,1\}}^{(2)}}(x_1,x_2) = \left(1,\ x_1,\ x_2,\ x_1^2,\ x_1x_2,\ x_2^2,\ x_1^3,\ x_1x_2^2,\ x_2^3,\ x_1^2x_2\right)^{\mathsf{T}}.$$

   with the targeted monomial $x_1^2x_2$ as the last element.

3. $k = 3$: $\mathbf{j}^{(3)}_{\{1,2\}} = (1,2)$, $|\mathbf{j}^{(3)}_{\{1,2\}}| = 3$

$$\mathcal{I}_{\{1,2\},|\mathbf{j}^{(3)}_{\{1,2\}}|} = \{(0,0),\ (1,0),\ (0,1),\ (2,0),\ (1,1),\ (0,2),\ (3,0),\ (2,1),\ (0,3),\ (1,2)\},\ \left|\mathcal{I}_{\{1,2\},|\mathbf{j}^{(3)}_{\{1,2\}}|}\right| = 10,$$

$$\mathbf{P}_{\{1,2\}\mathbf{j}^{(3)}_{\{1,2\}}}(x_1,x_2) = \left(1,\ x_1,\ x_2,\ x_1^2,\ x_1x_2,\ x_2^2,\ x_1^3,\ x_1^2x_2,\ x_2^3,\ x_1x_2^2\right)^{\mathsf{T}}.$$

with the targeted monomial $x_1x_2^2$ as the last element.

Consider the case of $k = 3$, where $\mathbf{j}^{(3)}_{\{1,2\}} = (1,2)$ and the targeted monomial is $x_1x_2^2$. Using (8) from Step 3, the associated monomial moment matrix

$$\mathbf{G}_{\{1,2\}\mathbf{j}^{(3)}_{\{1,2\}}} = \begin{bmatrix}
1 & 0 & 0 & \frac{1}{16} & \frac{1}{80} & \frac{1}{16} & 0 & 0 & 0 & 0 \\
\frac{1}{16} & 0 & 0 & \frac{3}{256} & \frac{3}{1280} & \frac{27}{6400} & 0 & 0 & 0 & 0 \\
0 & \frac{1}{80} & \frac{1}{16} & 0 & 0 & 0 & \frac{3}{1280} & \frac{27}{6400} & \frac{3}{256} & \frac{3}{1280} \\
\frac{1}{16} & 0 & 0 & \frac{3}{256} & \frac{3}{1280} & \frac{27}{6400} & 0 & 0 & 0 & 0 \\
\frac{1}{80} & 0 & 0 & \frac{3}{1280} & \frac{27}{6400} & \frac{3}{1280} & 0 & 0 & 0 & 0 \\
\frac{1}{16} & 0 & 0 & \frac{27}{6400} & \frac{3}{1280} & \frac{3}{256} & 0 & 0 & 0 & 0 \\
0 & \frac{3}{256} & \frac{3}{1280} & 0 & 0 & 0 & \frac{15}{4096} & \frac{3}{4096} & \frac{231}{512000} & \frac{87}{102400} \\
0 & \frac{3}{1280} & \frac{27}{6400} & 0 & 0 & 0 & \frac{3}{4096} & \frac{87}{102400} & \frac{87}{102400} & \frac{231}{512000} \\
0 & \frac{3}{1280} & \frac{3}{256} & 0 & 0 & 0 & \frac{231}{512000} & \frac{87}{102400} & \frac{15}{4096} & \frac{3}{4096} \\
0 & \frac{27}{6400} & \frac{3}{1280} & 0 & 0 & 0 & \frac{87}{102400} & \frac{231}{512000} & \frac{3}{4096} & \frac{87}{102400}
\end{bmatrix}.$$

Following Cholesky factorization of $\mathbf{G}_{\{1,2\}\mathbf{j}^{(3)}_u}$ from Step 4, the whitening matrix

$$\mathbf{W}_{\{1,2\}\mathbf{j}^{(3)}_{\{1,2\}}} = \begin{bmatrix}
1 & 0 & 0 & 0 & 0 & 0 & 0 & 0 & 0 & 0 \\
0 & 4 & 0 & 0 & 0 & 0 & 0 & 0 & 0 & 0 \\
0 & -\sqrt{\frac{2}{3}} & 5\sqrt{\frac{2}{3}} & 0 & 0 & 0 & 0 & 0 & 0 & 0 \\
-\frac{1}{\sqrt{2}} & 0 & 0 & 8\sqrt{2} & 0 & 0 & 0 & 0 & 0 & 0 \\
0 & 0 & 0 & -4\sqrt{\frac{2}{3}} & 20\sqrt{\frac{2}{3}} & 0 & 0 & 0 & 0 & 0 \\
-\frac{1}{\sqrt{2}} & 0 & 0 & \frac{\sqrt{2}}{3} & -\frac{10\sqrt{2}}{3} & \frac{25\sqrt{2}}{3} & 0 & 0 & 0 & 0 \\
0 & -2\sqrt{6} & 0 & 0 & 0 & 0 & 32\sqrt{\frac{2}{3}} & 0 & 0 & 0 \\
0 & \frac{1}{\sqrt{3}} & -\frac{5}{\sqrt{3}} & 0 & 0 & 0 & -\frac{16}{\sqrt{3}} & \frac{80}{\sqrt{3}} & 0 & 0 \\
0 & 0 & -\frac{10\sqrt{2}}{3} & 0 & 0 & 0 & \frac{8\sqrt{2}}{27} & -\frac{20\sqrt{2}}{9} & \frac{500\sqrt{2}}{27} & 0 \\
0 & -3 & \frac{5}{3} & 0 & 0 & 0 & \frac{50}{27} & -\frac{170}{9} & -\frac{250}{27} & 50
\end{bmatrix}.$$

Finally, using (11) from Step 4, the orthogonal polynomial corresponding to the targeted monomial $x_1x_2^2$ is obtained as

$$\Psi_{\{1,2\}\mathbf{j}^{(3)}_{\{1,2\}}} = \Psi_{\{1,2\},(1,2)} = -3x_1 + \frac{5}{3}x_2 + \frac{50}{27}x_1^3 - \frac{170}{9}x_1^2x_2 - \frac{250}{27}x_2^3 + 50x_1x_2^2,$$

which is the last element of the polynomial set described by (19). Following similar procedures, the orthogonal polynomials for the targeted monomials x_1x_2 ($k = 1$) and $x_1^2x_2$ ($k = 2$) can be obtained as the first and second elements of the aforementioned polynomial set.

Appendix B. Results of Example 1

Tables B.1 and B.2 present the orthogonal polynomials for Example 1, generated using the four-step algorithm and the Rodrigues formula, respectively.

Table B.1
Approximate orthogonal polynomials consistent with the three PDFs of Example 1.

Case 1: Gaussian PDF on $\mathbb{R}^3$ ($\sigma_1 = \sigma_2 = \sigma_3 = 1/4, \rho_{12} = \rho_{13} = \rho_{23} = 1/5$)
$\Psi_{\{0\},(0)} = 1,$
$\tilde{\Psi}_{\{i\},(1)} \approx 4.0000x_i,$
$\tilde{\Psi}_{\{i\},(2)} \approx -0.7071 + 11.3137x_i^2,$
$\tilde{\Psi}_{\{i\},(3)} \approx -4.8990x_i + 26.1279x_i^3,$
$\tilde{\Psi}_{\{i_1,i_2\},(1,1)} \approx 0.1961 - 3.2686x_{i_1}^2 - 3.2686x_{i_2}^2 + 16.9967x_{i_2}x_{i_1},$
$\tilde{\Psi}_{\{i_1,i_2\},(2,1)} \approx 1.6667x_{i_1} - 3.0000x_{i_2} - 9.2593x_{i_1}^3 + 50.0000x_{i_1}^2x_{i_2} + 1.8519x_{i_2}^3 - 18.8889x_{i_1}x_{i_2}^2,$
$\tilde{\Psi}_{\{i_1,i_2\},(1,2)} \approx -3.0000x_{i_1} + 1.6667x_{i_2} + 1.8519x_{i_1}^3 - 18.8889x_{i_1}^2x_{i_2} - 9.2593x_{i_2}^3 + 50.0000x_{i_1}x_{i_2}^2,$
$\tilde{\Psi}_{\{1,2,3\},(1,1,1)} \approx 0.4439x_1 + 0.4439x_2 + 0.4439x_3 + 1.9024x_1^3 - 9.8291x_1^2x_2 - 9.8291x_1^2x_3 - 9.8291x_1x_2^2 - 9.8291x_1x_3^2 + 1.9024x_2^3 - 9.8291x_2^2x_3 - 9.8291x_2x_3^2 + 1.9024x_3^3 + 73.5600x_1x_2x_3.$
Case 2: Gegenbauer PDF on the unit ball $\mathbb{B}^3$ ($\mu = 5$)
$\Psi_{\{0\},(0)} = 1,$
$\tilde{\Psi}_{\{i\},(1)} \approx 3.7417x_i,$
$\tilde{\Psi}_{\{i\},(2)} \approx -0.7845 + 10.9825x_i^2,$
$\tilde{\Psi}_{\{i\},(3)} \approx -5.3923x_i + 28.7590x_i^3,$
$\tilde{\Psi}_{\{i_1,i_2\},(1,1)} \approx 14.9984x_{i_1}x_{i_2},$
$\tilde{\Psi}_{\{i_1,i_2\},(2,1)} \approx -3.6522x_{i_2} + 3.6522x_{i_2}^3 + 47.7229x_{i_1}^2x_{i_2},$
$\tilde{\Psi}_{\{i_1,i_2\},(1,2)} \approx -3.6522x_{i_1} + 3.6522x_{i_1}^3 + 47.7229x_{i_1}x_{i_2}^2,$
$\tilde{\Psi}_{\{1,2,3\},(1,1,1)} \approx 63.4996x_1x_2x_3$
Case 3: Dirichlet PDF on the tetrahedron $\mathbb{T}^3$ ($k_1 = k_2 = k_3 = k_4 = 1$)
$\Psi_{\{0\},(0)} = 1,$
$\tilde{\Psi}_{\{i\},(1)} \approx -1.5273 + 6.1098x_i,$
$\tilde{\Psi}_{\{i\},(2)} \approx 2.0222 - 18.8756x_i + 30.2020x_i^2,$
$\tilde{\Psi}_{\{i\},(3)} \approx -2.5055 + 40.0937x_i - 144.3470x_i^2 + 137.4786x_i^3,$
$\tilde{\Psi}_{\{i_1,i_2\},(1,1)} \approx 4.4616 - 20.8161x_{i_1} - 20.8161x_{i_2} + 16.3546x_{i_1}^2 + 16.3546x_{i_2}^2 + 56.5066x_{i_1}x_{i_2},$
$\tilde{\Psi}_{\{i_1,i_2\},(2,1)} \approx -7.2106 + 69.7704x_{i_1} + 45.6315x_{i_2} - 156.5890x_{i_1}^2 - 315.5668x_{i_1}x_{i_2} - 69.6313x_{i_2}^2 + 94.1290x_{i_1}^3 + 245.7964x_{i_1}x_{i_2}^2 + 31.2103x_{i_2}^3 + 385.4555x_{i_1}^2x_{i_2},$
$\tilde{\Psi}_{\{i_1,i_2\},(1,2)} \approx -7.2106 + 45.6315x_{i_1} + 69.7704x_{i_2} - 69.6313x_{i_1}^2 - 315.5668x_{i_1}x_{i_2} - 156.5890x_{i_2}^2 + 31.2103x_{i_1}^3 + 245.7964x_{i_1}^2x_{i_2} + 94.1290x_{i_2}^3 + 385.4555x_{i_1}x_{i_2}^2,$
$\tilde{\Psi}_{\{1,2,3\},(1,1,1)} \approx -26.6996 + 142.3955x_1 + 142.3947x_2 + 142.4017x_3 - 204.6920x_1^2 - 513.2261x_1x_2 - 513.2261x_1x_3 - 204.6891x_2^2 - 513.2261x_2x_3 - 204.6891x_3^2 + 88.9962x_1^3 + 370.8128x_1^2x_2 + 370.8244x_1^2x_3 + 370.8106x_1x_2^2 + 370.8366x_1x_3^2 + 88.9962x_2^3 + 370.8211x_2^2x_3 + 370.8382x_2x_3^2 + 88.9962x_3^3 + 949.2981x_1x_2x_3,$

a. Here, $i \in \{1,2,3\}$ and $i_1, i_2 \in \{1,2,3\}$ with $i_2 > i_1$.

Table B.2
Exact orthogonal polynomials consistent with the three PDFs of Example 1.

Case 1: Gaussian PDF on $\mathbb{R}^3$ ($\sigma_1 = \sigma_2 = \sigma_3 = 1/4, \rho_{12} = \rho_{13} = \rho_{23} = 1/5$)
$\Psi_{\{0\},(0)} = 1,$
$\Psi_{\{i\},(1)} \approx 4x_i,$
$\Psi_{\{i\},(2)} \approx -0.7071 + 11.3137x_i^2,$
$\Psi_{\{i\},(3)} \approx -4.8990x_i + 26.1279x_i^3,$
$\Psi_{\{i_1,i_2\},(1,1)} \approx 0.1961 - 3.2686x_{i_1}^2 - 3.2686x_{i_2}^2 + 16.9967x_{i_2}x_{i_1},$
$\Psi_{\{i_1,i_2\},(2,1)} \approx 1.6667x_{i_1} - 3x_{i_2} - 9.2593x_{i_1}^3 + 50x_{i_1}^2x_{i_2} + 1.8519x_{i_2}^3 - 18.8889x_{i_1}x_{i_2}^2,$
$\Psi_{\{i_1,i_2\},(1,2)} \approx -3x_{i_1} + 1.6667x_{i_2} + 1.8519x_{i_1}^3 - 18.8889x_{i_1}^2x_{i_2} - 9.2593x_{i_2}^3 + 50x_{i_1}x_{i_2}^2,$
$\Psi_{\{1,2,3\},(1,1,1)} \approx 0.4439x_1 + 0.4439x_2 + 0.4439x_3 + 1.9024x_1^3 - 9.8291x_1^2x_2 - 9.8291x_1^2x_3 - 9.8291x_1x_2^2 - 9.8291x_1x_3^2$ $+1.9024x_2^3 - 9.8291x_2^2x_3 - 9.8291x_2x_3^2 + 1.9024x_3^3 + 73.5600x_1x_2x_3.$
Case 2: Gegenbauer PDF on the unit ball $\mathbb{B}^3$ ($\mu = 5$)
$\Psi_{\{0\},(0)} = 1,$
$\Psi_{\{i\},(1)} \approx -3.7417x_i,$
$\Psi_{\{i\},(2)} \approx -0.7845 + 10.9825x_i^2,$
$\Psi_{\{i\},(3)} \approx 5.3923x_i - 28.7589x_i^3,$
$\Psi_{\{i_1,i_2\},(1,1)} \approx 14.9666x_{i_1}x_{i_2},$
$\Psi_{\{i_1,i_2\},(2,1)} \approx 3.5949x_{i_2} - 3.5949x_{i_2}^3 - 46.7332x_{i_1}^2x_{i_2},$
$\Psi_{\{i_1,i_2\},(1,2)} \approx 3.5949x_{i_1} - 3.5949x_{i_1}^3 - 46.7332x_{i_1}x_{i_2}^2,$
$\Psi_{\{1,2,3\},(1,1,1)} \approx -63.4980x_1x_2x_3$
Case 3: Dirichlet PDF on the tetrahedron $\mathbb{T}^3$ ($k_1 = k_2 = k_3 = k_4 = 1$)
$\Psi_{\{0\},(0)} = 1,$
$\Psi_{\{i\},(1)} \approx 1.5275 - 6.1101x_i,$
$\Psi_{\{i\},(2)} \approx 2.0225 - 18.8776x_i + 30.2042x_i^2,$
$\tilde{\Psi}_{\{i\},(3)} \approx 2.5064 - 40.1024x_i + 144.3688x_i^2 - 137.4941x_i^3,$
$\Psi_{\{i_1,i_2\},(1,1)} \approx 4.4604 - 20.8149x_{i_1} - 20.8149x_{i_2} + 16.3546x_{i_1}^2 + 16.3546x_{i_2}^2 + 56.4978x_{i_1}x_{i_2},$
$\Psi_{\{i_1,i_2\},(2,1)} \approx 7.2019 - 69.6181x_{i_1} - 45.6118x_{i_2} + 156.0405x_{i_1}^2 + 315.2819x_{i_1}x_{i_2} + 69.6181x_{i_2}^2 - 93.6243x_{i_1}^3$ $-245.6638x_{i_1}x_{i_2}^2 - 31.2081x_{i_2}^3 - 384.8999x_{i_1}^2x_{i_2},$
$\Psi_{\{i_1,i_2\},(1,2)} \approx 7.2019 - 45.6118x_{i_1} - 69.6181x_{i_2} + 69.6181x_{i_1}^2 + 315.2819x_{i_1}x_{i_2} + 156.0405x_{i_2}^2 - 31.2081x_{i_1}^3$ $-245.6638x_{i_1}^2x_{i_2} - 93.6243x_{i_2}^3 - 384.8999x_{i_1}x_{i_2}^2,$
$\Psi_{\{1,2,3\},(1,1,1)} \approx 26.6983 - 142.3910x_1 - 142.3910x_2 - 142.3910x_3 + 204.6871x_1^2 + 513.2009x_1x_2 + 513.2009x_1x_3 + 204.6871x_2^2$ $+513.2009x_2x_3 + 204.6871x_3^2 - 88.9944x_1^3 - 370.8099x_1^2x_2 - 370.8099x_1^2x_3 - 370.8099x_1x_2^2 - 370.8099x_1x_3^2$ $-88.9944x_2^3 - 370.8099x_2^2x_3 - 370.8099x_2x_3^2 - 88.9944x_3^3 - 949.2734x_1x_2x_3,$

a. Here, $i \in \{1, 2, 3\}$ and $1 \le i_1 < i_2 \le 3$.
b. The orthogonal polynomials are computed exactly; only round-off error is incurred.

References

[1] N. Wiener, The homogeneous chaos, Am. J. Math. 60 (4) (1938) 897–936.
[2] R.H. Cameron, W.T. Martin, The orthogonal development of non-linear functionals in series of Fourier–Hermite functionals, Ann. Math. 48 (1947) 385–392.
[3] G. Blatman, B. Sudret, Adaptive sparse polynomial chaos expansion based on least angle regression, J. Comput. Phys. 230 (2011) 2345–2367.
[4] S. Rahman, A polynomial dimensional decomposition for stochastic computing, Int. J. Numer. Methods Eng. 76 (2008) 2091–2116.
[5] S. Rahman, Mathematical properties of polynomial dimensional decomposition, SIAM/ASA J. Uncert. Quantific. 6 (2018) 816–844.
[6] I. Babuska, F. Nobile, R. Tempone, A stochastic collocation method for elliptic partial differential equations with random input data, SIAM J. Numer. Anal. 45 (3) (2007) 1005–1034.
[7] X. Ma, N. Zabaras, An adaptive hierarchical sparse grid collocation algorithm for the solution of stochastic differential equations, J. Comput. Phys. 228 (2009) 3084–3113.
[8] S. Smolyak, Quadrature and interpolation formulas for tensor products of certain classes of functions, Dokl. Akad. Nauk SSSR 4 (1963) 240–243.
[9] T. Gerstner, M. Griebel, Numerical integration using sparse grids, Numer. Algorithms 18 (1998) 209–232.
[10] Y. Noh, K.K. Choi, L. Du, Reliability-based design optimization of problems with correlated input variables using a gaussian copula, Struct. Multidiscip. Optim. 38 (2009) 1–16.
[11] M. Rosenblatt, Remarks on a multivariate transformation, Ann. Math. Statist. 23 (1952) 470–472.
[12] M. Arnst, R. Ghanem, E. Phipps, J. Red-Horse, Measure transformation and efficient quadrature in reduced-dimensional stochastic modeling of coupled problems, Int. J. Numer. Methods Eng. 92 (2012) 1044–1080.
[13] L. Mehrez, J. Fish, V. Aithraju, W. Rodgers, R. Ghanem, A PCE-based multiscale framework for the characterization of uncertainties in complex systems, Comput. Mech. 61 (2018) 219–236.
[14] S. Rahman, A polynomial chaos expansion in dependent random variables, J. Appl. Math. Appl. 4 (2018) 1–26.
[15] S. Rahman, Uncertainty quantification under dependent random variables by a generalized polynomial dimensional decomposition, Comput. Methods Appl. Mech. Eng. 344 (2019) 910–937.
[16] S. Rahman, Dimension-wise multivariate orthogonal polynomials in general probability spaces, Appl. Math. Comput. 362 (2019) 1–19.
[17] C. Soize, R. Ghanem, Physical systems with random uncertainties: chaos representations with arbitrary probability measures, SIAM J. Sci. Comput. 26 (12) (2004) 395–410.
[18] X. Zeng, R. Ghanem, Data-driven projection pursuit adaptation of polynomial chaos expansions for dependent high-dimensional parameters, Comput. Methods Appl. Mech. Eng. 433 (2025). .
[19] C.F. Dunkl, Y. Xu, Orthogonal Polynomials of Several Variables, Encyclopedia of Mathematics and its Applications 155, Cambridge University Press, 2nd edition, 2001.
[20] G.H. Golub, C.F. van Loan, Matrix Computations, The John Hopkins University Press, third edition, 1996.
[21] T.H. Koornwinder, Two-variable analogues of the classical orthogonal polynomials, in theory and applications of special functions (1975).
[22] P. Appell, J.K. de Fériet, Fonctions hyprgéométriques et hypersphériques, polynomes d'Hermite (1926) 1–14.
[23] A. Erdélyi, Higher Transcendental Functions, II of *Encyclopedia of Mathematics and its Applications 155*, McGraw-Hill, 1953.
[24] H.L. Krall, I.M. Sheffer, Orthogonal polynomials in two variables, Ann. Mat. Pura Appl. 76 (4) (1967) 325–376.

[25] B. Holmquist, The d-variate vector hermite polynomial of order k, Linear Algebra Appl. 237-238 (1996) 155–190.
[26] A. Kessy, A. Lewin, K. Strimmer, Optimal whitening and decorrelation, Am. Stat. (2018). https://doi.org/10.1080/00031305.2016.1277159
[27] J.M. Taylor, The condition of gram matrices and related problems, Proc. R. Soc. Edinburgh 80A (1978) 45–56.
[28] S. Rahman, A generalized ANOVA dimensional decomposition for dependent probability measures, SIAM/ASA J. Uncert. Quantific. 2 (2014) 670–697.
[29] G. Hooker, Generalized functional ANOVA diagnostics for high-dimensiobal functions of dependent variables, J. Comput. Graph. Stat. 16 (3) (2007) 709–732.
[30] W.J. Morokoff, R.E. Caflisch, Quasi-Monte Carlo integration, J.Comput. Phys. 122 (1995) 218–230.
[31] D. Lee, S. Rahman, Practical uncertainty quantification analysis involving statistically dependent random variables, Appl. Math. Model. 84 (2020) 324–356.
[32] W. Gautschi, Orthogonal Polynomials: Computation and Approximation, Numerical Mathematics and Scientific Computation, Oxford University Press, 2004.
[33] S. Rahman, Extended polynomial dimensional decomposition for arbitrary probability distributions, J. Eng. Mech. 135 (12) (2009) 1439–1451.
[34] H.O. Madsen, S. Krenk, N.C. Lind, Methods of Structural Safet, Prentice-Hal, 1986.
[35] Abaqus Standard, Version 2024, Dassault Systems Simulia Corp., 2024.
[36] R. Bellman, Dynamic Programming, Princeton University Press Princeton, NJ, 1957.